



**ANKARA YILDIRIM BEYAZIT UNIVERSITY
GRADUATE SCHOOL OF NATURAL AND APPLIED SCIENCES**

**HIGH PERFORMANCE AUTOMATED DIAGNOSIS SYSTEM FOR
HYPERTENSIVE RETINOPATHY**

**M.Sc. Thesis by
Zülbiye AKÇA**

Department of Computer Engineering

May, 2017

ANKARA

HIGH PERFORMANCE AUTOMATED DIAGNOSIS SYSTEM FOR HYPERTENSIVE RETINOPATHY

**A Thesis Submitted to
the Graduate School of Natural and Applied Sciences of Ankara Yıldırım
Beyazıt University**

**In Partial Fulfillment of the Requirements for the Degree of Master of Science
in Computer Engineering, Department of Computer Engineering**

by

Zülbiye AKÇA

May, 2017

ANKARA

M.Sc THESIS EXAMINATION RESULT FORM

We have read the thesis entitled “HIGH PERFORMANCE AUTOMATED DIAGNOSIS SYSTEM FOR HYPERTENSIVE RETINOPATHY” completed by Zülbiye AKÇA under supervision of Asst. Prof. Dr. Baha ŞEN and we certify that in our opinion it is fully adequate, in scope and in quality, as a thesis for the degree of Master of Science.

Asst. Prof. Dr. Baha ŞEN

(Supervisor)

Prof. Dr. Şahin EMRAH

(Jury Member)

Prof. Dr. Fatih V. ÇELEBİ

(Jury Member)

Prof. Dr. Fatih V. ÇELEBİ

(Director)

Graduate School of Natural and Applied Sciences

ETHICAL DECLARATION

I have prepared this dissertation study in accordance with the Rules of Writing Thesis of Ankara Yıldırım Beyazıt University of Science and Technology Institute;

- Data I have presented in the thesis, information and documents that I obtained in the framework of academic and ethical rules,
- All information, documentation, assessment and results that I presented in accordance with scientific ethics and morals,
- I have gave references all the works that I were benefited in this dissertation by appropriate reference,
- I would not make any changes in the data I were used,
- The work presented in this dissertation I would agree that the original,

I state, in the contrary case I declare that I accept the all rights losses that may arise against me.

HIGH PERFORMANCE AUTOMATED DIAGNOSIS SYSTEM FOR HYPERTENSIVE RETINOPATHY

ABSTRACT

High blood pressure (hypertension), defined as the rise of blood pressure, can cause serious damage to the human body, which can lead to death. One of the devastating effects of hypertension is on retina of the eye. This vascular problem which is causing retinal deterioration is called “Hypertensive Retinopathy”. Hypertensive retinopathy, which is characterized by thickening or narrowing of the retinal vessels, may result in vision loss and even blindness in later stages of the disease if it is not diagnosed and treated early. To detect presence of hypertensive retinopathy, retinal images must be examined in detail by eye specialists but making these examinations manually may take a lot of time and lead to false diagnosis. For this reason, intelligent computer systems that produce automatic and fast results for these diagnoses procedures are required. The aim of this thesis is to be able to diagnose hypertensive retinopathy with high accuracy and high performance. Firstly, blood vessels in the retinal images that are taken from publicly available DRIVE and STARE databases are segmented for making examination in detail by applying a set of image processing methods. The Arteriovenous Ratio (AVR) is used to detect and calculate changes in the segmented blood vessels due to hypertensive retinopathy. It is decided whether there is hypertensive retinopathy according to the calculated AVR value for each retinal image. These operations that are applied on the retinal images for the diagnosis of hypertensive retinopathy are time consuming procedures. Therefore, improvements that are done on the Graphical Processing Unit (GPU) make it possible to perform diagnosis operations in a much shorter time and without compromising accuracy.

Keywords: hypertensive retinopathy, AVR, high performance system, image processing, image segmentation, image enhancement, GPU.

GÖZ TANSİYONUNUN TESPİTİ İÇİN YÜKSEK PERFORMANSLI TANI SİSTEMİ

ÖZET

Kan basıncının yükselmesi olarak tanımlanan, yüksek tansiyon (hipertansiyon) insan vücudu üzerinde ölüme kadar varabilen ciddi hasarlara sebep olabilmektedir. Hipertansiyonun yıkıcı etkilerinden birisi de göz dolayısıyla retina üzerinde olmaktadır. Retinada bozulmaya neden olan bu damarsal sorun hipertansif retinopati olarak adlandırılır. Retina damarlarında kalınlaşma, daralma gibi belirtiler gösteren hipertansif retinopati erken teşhis ve tedavi edilmediğinde hastalığın ilerleyen dönemlerinde görme kaybına ve hatta körlüğe bile neden olabilmektedir. Bu nedenle göz uzmanları tarafından retina görüntülerinin detaylı olarak incelenmesi gerekmektedir. Bu incelemelerin manuel olarak yapılması zaman alan işlemlerdir. Ayrıca elle yapılan bu değerlendirmede hatalı kararlar verilebilmektedir. Bu nedenle bu tanı ve teşhis işlemleri için otomatik ve hızlı sonuçlar üreten akıllı bilgisayar sistemlerine ihtiyaç duyulmaktadır. Bu tez kapsamında yapılan çalışmalarla hipertansif retinopatinin yüksek doğruluk ve hızlı çalışan bir sistem ile tanılanabilmesi amaçlanmıştır. DRIVE ve STARE veri tabanlarından alınan test retina görüntülerine bir takım görüntü işleme yöntemleri uygulanarak retina görüntüsü üzerindeki kan damarları bulunarak atardamar ve toplardamar olarak ayrıştırılmıştır. Ayrıştırılan damarlarda hipertansif retinopatiden kaynaklanan değişimlerin tespit edilip hesaplanabilmesi için atar damar-toplardamar oranı (Arteriovenous Ratio AVR) kullanılmıştır. Her bir retina görüntüsü için hesaplanan AVR değerine göre hipertansif retinopatinin olup olmadığına karar verilmiştir. Hipertansif retinopati tanısı için retina görüntüsü üzerinde yapılan işlemler zaman alan işlemlerdir. Harcanan bu zamanın azaltılarak, kısa sürede ve hassasiyetten ödün vermeden teşhis işlemlerinin yapılabilmesi “Grafik İşlemci Birimi” (GİB) üzerinde yapılan geliştirmelerle sağlanmıştır.

Anahtar kelimeler: göz tansiyonu, DTO, görüntü işleme, görüntü iyileştirme, görüntü bölütleme, yüksek performanslı sistem, GİB.

ACKNOWLEDGEMENTS

I would like to take this opportunity to thank my tutor and supervisor Asst. Prof. Dr. Baha ŐEN and for his support, guidance, encouragement and enthusiasm he showed from the initial stages to the end of the project. It has been an honor and a pleasure for me to work with him.

Also, I would like to thank my dear husband Eren AKŐA for his great support and my family for being with me all the way.

2017, 08 May

Zülbiye AKŐA

CONTENTS

M.Sc THESIS EXAMINATION RESULT FORM.....	ii
ETHICAL DECLARATION.....	iii
ABSTRACT.....	iv
ÖZET	v
ACKNOWLEDGEMENTS	vi
CONTENTS	vii
ABBREVIATIONS	ix
LIST OF TABLES.....	x
LIST OF FIGURES.....	xi
CHAPTER 1 – INTRODUCTION.....	1
1.1 Basic Knowledge for Hypertensive Retinopathy.....	2
1.1.1 Classification and Diagnosis of Hypertensive Retinopathy	4
1.1.2 Arteriovenous Ratio (AVR)	4
1.2 Related Works.....	5
CHAPTER 2 – MATERIAL AND METHODS.....	9
2.1 Retinal Image Databases.....	9
2.1.1 DRIVE.....	9
2.1.2 STARE	10
2.2 Retinal Image Pre-processing.....	11
2.3 Retinal Image Segmentation.....	13
2.4 Extraction of Region of Interest.....	14
2.4.1 Mathematical Morphology	15
2.4.2 Canny Edge Detection	16
2.4.3 Circular Hough Transform	17
2.5 Image Processing with MATLAB	18
2.6 Parallel Computing on GPUs with MATLAB	19
2.6.1 GPU-enabled built-in Image Processing Functions	21
2.6.2 arrayfun on gpuArray.....	22
2.6.3 CUDA Kernel.....	22

CHAPTER 3 – IMPLEMENTATION	24
3.1 Implementation Architecture	24
3.2 Pre-processing.....	26
3.3 Blood Vessel Segmentation	30
3.4 Finding Region of Interest.....	33
3.5 Measurement of the Diameter of Blood Vessels and AVR.....	40
CHAPTER 4 - RESULTS AND DISCUSSION	47
4.1 Blood Vessel Segmentation	47
4.2 Detection of Optic Disc Location.....	50
4.3 Diagnosis of Hypertensive Retinopathy.....	52
4.4 GPU Optimized Results	53
CHAPTER 5 – CONCLUSION AND FUTURE WORKS	55
REFERENCES.....	57
RESUME	64

ABBREVIATIONS

RGB	Red, Green, Blue
HR	Hypertensive Retinopathy
CLAHE	Contrast Limited Adaptive Histogram Equalization
OD	Optic Disc
ROI	Region of Interest
DRIVE	Digital Retinal Images for Vessel Extraction
STARE	Structured Analysis of the Retina
AVR	Arteriovenous Ratio
IPT	Image Processing Toolbox
PCT	Parallel Computing Toolbox
GPU	Graphical Processing Unit
CPU	Central Processing Unit
CUDA	Compute Unified Device Architecture
HSI	Hue, Saturation, Intensity
CRAE	Central Artery Equivalent
CRVE	Central Vein Equivalent

LIST OF TABLES

Table 1.1 Keith-Wagener-Barker classification for Hypertensive Retinopathy [5]	4
Table 3.1 Keith-Wagener-Barker AVR values to diagnose HR	46
Table 4.1 Parameters of performance measures	48
Table 4.2 Accuracy calculations for all images from DRIVE database	49



LIST OF FIGURES

Figure 1.1 The main parts of the human eye [1]	2
Figure 1.2 Anatomical structure of fundus image [2].....	3
Figure 2.1 Sample from DRIVE database (a) The original image (b) The mask of an original image (c) Manual segmentation of blood vessels	10
Figure 2.2 Sample from STARE database (a) The original image (b) Manual segmentation by first observer (c) Manual segmentation of blood vessels by second observer	10
Figure 2.3 (a) Histogram of original image (b) Original image (c) Histogram of equalized image (d) Histogram equalized image [26]	12
Figure 2.4 Morphological operators (a) Erosion (b) Dilation	16
Figure 2.5 The working principle of data parallelism	20
Figure 2.6 Hardware architectures of CPU and GPU	20
Figure 2.7 GPU-enabled imfilter function	22
Figure 2.8 CUDA Kernel	23
Figure 3.1 Steps of the proposed method	25
Figure 3.2 CUDA device properties	26
Figure 3.3 Pre-processing steps.....	27
Figure 3.4 (a) Red channel (b) Green channel (c) Blue channel	27
Figure 3.5 Comparison of grayscale and green channel (a) Original image (b) Grayscale image (c) Green channel image.....	28
Figure 3.6 Comparison of Global HE and CLAHE (a) Green channel (b) Histogram of green channel (c) Global HE is applied (d) Histogram of Global HE (e) CLAHE is applied (f) Histogram of CLAHE.....	29
Figure 3.7 Blood vessel segmentation steps.....	30
Figure 3.8 Retinal image background exclusion (a) Input image (b) Average filtered image (c) Background excluded image.....	31

Figure 3.9 Segmentation results (a) DRIVE database hand-labelled segmentation (b) Segmentation with Otsu’s method (c) Segmentation with iterative thresholding method	33
Figure 3.10 Extraction of ROI.....	34
Figure 3.11 Morphological closing implementation on GPU	36
Figure 3.12 The result of morphological closing operation.....	37
Figure 3.13 The detected edges with Canny’s method.....	38
Figure 3.14 The detected circular shapes with Circular Hough Transform	38
Figure 3.15 The detected optic disc	39
Figure 3.16 The pseudocode for finding region of interest.....	40
Figure 3.17 (a) Image with vessels edge points (b) Image with vessels centerline points.....	41
Figure 3.18 Flow diagram of discovering vessels around the center of optic disc.....	42
Figure 3.19 Measurement of vessel diameter.....	44
Figure 3.20 Flow diagram of vessel width calculation.....	45
Figure 4.1 Optic disc detection results for images from DRIVE database.....	51
Figure 4.2 Classification result for images labelled image as HR in STARE database	52
Figure 4.3 Classification result for images labelled as normal (non-HR) in STARE database	53
Figure 4.4 The graphical representation of running times on GPU and CPU.....	54

CHAPTER 1

INTRODUCTION

High blood pressure can cause an abnormality of the retina that is called as “Hypertensive Retinopathy (HR)”. Early diagnosis of this disease is a difficult and sensitive procedure, and if it is not treated early, the disease causes severe damage in the following periods. Late diagnoses can lead loss of vision and even blindness in the patients. For this reason, it is vital that the disease is detected before it reaches the future stages. The most prominent feature used in the diagnosis of hypertensive retinopathy is the narrowing of the arteries. Determination of the level of arterial narrowing is possible by detecting arteries, veins and measuring their diameters. Different image processing algorithms are needed to be applied to retinal images in order to classify vessels and measure their thickness. These image processing algorithms can be thought as image enhancement, segmentation, finding region of interest and classification.

In the scope of this thesis, it is aimed that the diagnosis of hypertensive retinopathy can be made without compromising the accuracy and at high speed Graphical Processing Units (GPUs). The researches, studies and implementations to achieve this aim are explained in the following manner. In the following sections of this chapter, some basic knowledge about hypertensive retinopathy is provided briefly and the related works in the literature are discussed. In Chapter 2, the researches that are done for this study and the methods and algorithms that are used to diagnose hypertensive retinopathy are elaborated with CPU and GPU implementations. Chapter 3 describes implementation that is carried out in this study and experimental results and discussion about them are mentioned in Chapter 4. In the last chapter, this work is concluded and improvements and developments to be made in the next period are explained.

1.1 Basic Knowledge for Hypertensive Retinopathy

The eye is the most complex organ in the human body. The ability of the brain to perceive images is provided by the eye by converting light signals into electrical signals which are transmitted to the brain via optic nerves. Various parts of the eye play important roles in the working mechanism of the eye. These parts are shown in Figure 1.1 [1].

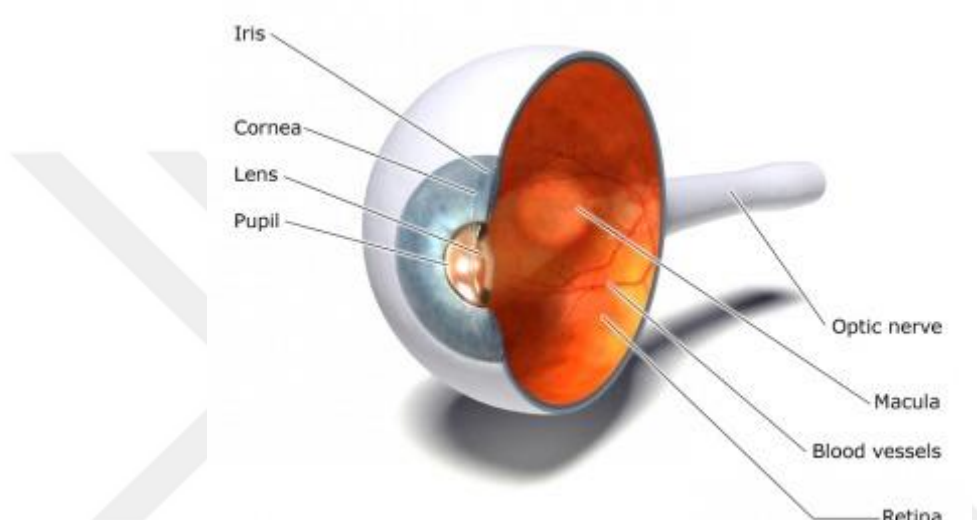


Figure 1.1 The main parts of the human eye [1].

The retina is a third and an inner part of layered eye structure. Images of the visual world are transferred to the retina using the cornea and lens. The retina is responsible for converting incoming light into a neural signal to send them to the brain. It works like a camera with sensory cells located in it. Because of the importance of retina, retinal images are used in the diagnosis and treatment of different eye diseases. The retinal images obtained using a fundus camera, are made available for analysis by ophthalmologists using several image processing and pattern recognition methods. It is possible to evaluate the presence of different diseases and to determine the stage of disease by analyzing the parts of the fundus images such as blood vessels, optic disc and fovea. Figure 1.2 shows fundus image with its anatomical structure [2].

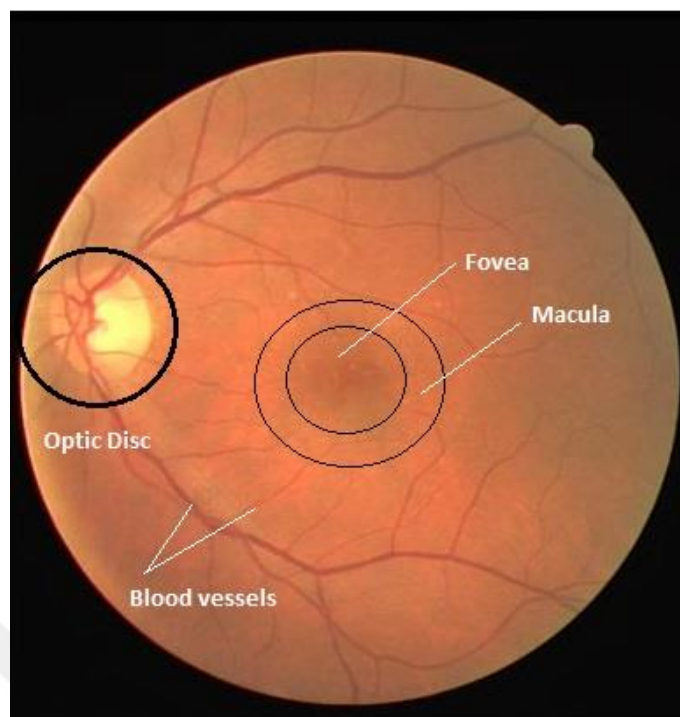


Figure 1.2 Anatomical structure of fundus image [2].

The optic disc (OD) is a bright yellowish circular disk that optic nerves emerge. It is also the entry point of the main blood vessels that feed retina. Determination of the location of the optic disc in retinal image analysis is a significant issue. Its diameter is usually used as a reference length to measure distances and sizes. For example; optic disc is used to determine approximate location of the fovea or center of vision. Examinations that are made on the optic disc are used to examine the current state of certain diseases and the severity of them. In the study of retinal diseases, blood vessels are also important. Blood vessels composed of arteries and veins are responsible for transporting blood to the internal structures of the eye. Because of systemic and local ocular disease, blood vessels may show measurable abnormalities in diameter, color and tortuosity. For instance; retinal artery occlusion may cause generalized arteriolar narrowing, hypertension also leads to generalized or focal arteriolar narrowing [3].

Hypertension, also known as high blood pressure, is a disease in which arterial blood pressure rises persistently. It causes various health problems such as heart disease, as well as retinal circulation also suffers from several systemic changes due to high

blood pressure such as long term damage to the retina. These systemic changes are clinically named as Hypertensive Retinopathy [4].

1.1.1 Classification and Diagnosis of Hypertensive Retinopathy

The accurate classification of grade of hypertensive retinopathy from a retinal image is important because it results in worse outcomes at each grade of it. In Table 1.1, Keith-Wagner-Barker classification for hypertensive retinopathy is represented.

Table 1.1 Keith-Wagener-Barker classification for Hypertensive Retinopathy [5].

Grade	Features
I	Mild generalised retinal arteriolar narrowing
II	Definite focal narrowing and arteriovenous nipping
III	Signs of grade II plus and retinal haemorrhages, exudates and cotton-wool spots
IV	Severe grade III plus papilloedema

Grade 1 is also known as mild hypertensive retinopathy which is weakly related with cardiovascular diseases. Grade 2 may result in heart failure, stroke and cardiovascular mortality which can be named as moderate hypertensive retinopathy. Grade 3 is a combination of grade 1 and grade 2. Accelerated hypertensive retinopathy corresponds to grade 4 and it can cause renal failure and mortality [4]. Therefore, timely diagnosis and treatment of hypertensive retinopathy is vital.

It is possible to diagnose the disease with some changes in the retinal vessels such as thickening of arteries and changes in arteriovenous crossings. Therefore, measuring arteriovenous ratio can be used for diagnosis hypertensive retinopathy also for detecting the stages of hypertensive retinopathy.

1.1.2 Arteriovenous Ratio (AVR)

Hypertensive retinopathy causes several systemic changes that are reflected in the retinal blood vessels. The ophthalmologists need to examine retinal blood vessels to

be able to assess the presence of this disease. Vascular diameter is one of the most important features used in diagnosing hypertensive retinopathy. Therefore, early detection of hypertensive retinopathy may be possible by measuring arteriovenous ratio (AVR), which is indicative of arterial narrowing. Estimation of AVR is done by using the diameters of specific arterioles and venules in the region around the optic disc. According to the obtained AVR values, a lower AVR (narrower arteriolar caliber) value is associated with a high blood pressure [6].

For AVR value to be measured correctly, the features of the arteries and veins on the retinal image should be well known. There are basically four different ways to separate arteries from veins [7].

- Arteries are brighter than veins.
- Arteries are thinner than neighboring veins.
- The central reflex (light reflex of the inner parts of the vessels) wider in the arteries and smaller in the veins.
- Before the arteries and veins branching out, they alternate near the optic disc in general (one artery is next to two veins).

1.2 Related Works

Detecting hypertensive retinopathy from retinal fundus image is a challenging task. This process includes finding and measuring the properties of blood vessels such as width, length. There are number of work is suggested in the literature to diagnose hypertensive retinopathy by segmenting and analyzing retinal images. However, in many of these works that are recommended for HR diagnosis, the acceleration of applications is not taken into the consideration, so improvements of them are done only on the CPU.

G. C. Manikis et al [8] proposed a system for early diagnosis to HR. In this system, segmentation of blood vessels is performed by using multi-scale filtering technique for improving contrast between vessels and background and iterative thresholding method for segmenting blood vessel structure. Afterwards, width of vessels in the

region of interest is measured to calculate AVR. This proposed system is tested on DRIVE and STARE databases having accuracy of %93.71 and %93.18 respectively.

The other HR diagnosing methods are proposed method by M. R. Faheem et al [9]. In this method, retinal images are preprocessed to remove noise and blood vessels are segmented match filtering technique. Classification of blood vessels as arteries and veins neural network is used. After classification process, AVR is calculated by using measurement of blood vessels in the region of interest. DRIVE database is used for the sake of diagnosis of HR and %93.9 accuracy is obtained.

The support system is developed by K. Noronha et al [10] for the automated detection of HR. Radon transform is applied for the vessel segmentation. To obtain AVR, classification of blood vessels in the region of interest is needed. This region is detected by detecting optic disc using Hough transform. This work is conducted on DRIVE database and showed accuracy of %92 in segmenting blood vessels.

U. G. Abbasi et al [11] proposed method to detect HR in five major steps which are images acquisition, vessel extraction, ROI detection, AVR calculation and diagnosis step. In this paper, variance based method is used for separation of background from foreground. Using 2-D Gabor wavelet and Multilayer thresholding, vessels are enhanced. Different data mining classification techniques to classify blood vessels as arteries and veins are used and better accuracy is obtained from Support Vector Machine with %81 accuracy. Subsequently, AVR is calculated to decide whether HR is found or not and grading of it.

K. Narasimhan et al [12] proposed an algorithm which firstly segment the blood vessels. To classify blood vessels, intensity variation and color information obtained from extraction of gray level and moment based features. AVR is calculated by using estimation of vessel width, to determine the changes in vessel diameter and to grade the various stages of hypertensive retinopathy. In the result of this work, 22 images of 25 normal images are classified as normal and 72 images of 76 abnormal images are classified as abnormal.

J. Lowell et al [13] presented an algorithm to measure the vessel diameter with sub pixel accuracy. Measurement of vessel diameter is made by using 2-D Gaussian model. This algorithm gives more precise result when comparing HHFW, Gregson and a 1-D Gaussian. The standard deviation of width difference is obtained 0.34, 0.58, 0.62 and 0.84 respectively 2D model, 1D Gaussian, HHFW (Half-Height at Full-Width) and Gregson.

C. Muramatsu et al [14] developed retinal fundus image analyzer for diagnosis of hypertensive retinopathy. Retinal blood vessels are segmented using black top-hat transformation. A/V ratio calculation is done by using major retinal vessels and classifying them into arteries and veins. DRIVE database is used.

D. Ortiz et al [15] presented a method for calculating AVR. This calculation is done by measuring the vessel diameters by using Gabor wavelet, gradients, morphological operations and Niblack. MATLAB is preferred as a development tool. This proposed method is composed of five steps that are image pre-processing, image segmentation, ROI detection, arteries and veins classification and blood vessels measurement. This method is tested on 30 images that includes 21 images HR diagnosed by experts. This method successfully classified 17 images.

The fully automatic method to detect HR is presented by C. Agurto et al [16]. This method is based on specification of retinal vessel features in terms of tortuosity, texture, color and AVR and linear regression classification by using vessel features as inputs. With this way %80 accuracy is achieved in detecting HR.

In addition to these studies on the CPU to diagnose HR, some of the image processing methods that are related to retinal images are implemented on GPU. For example, retinal blood vessels are segmented based on the GPU by F. Argüello et al [17]. They are intended to propose fast and accurate technique for retinal vessel tree extraction. In this work, image filtering and contour tracing are used and proposed method is tested on DRIVE and STARE databases in an average of 14 ms and 18 ms respectively. They compared their method with other works and the good accuracy/performance rate is obtained.

Also, G. S. Torres et al [18] proposed an approach based on evolution strategy to detect optic disc and segment retinal images using GPU with CUDA. Coarse detection and contour edge refinement are main steps of algorithm. STARE and DIARECTDB databases are testing environment. They showed that %96 accuracy is achieved with 5x and 7x speedup when it is compared to implementation on CPU.

One of the main steps in processing retinal images is image enhancement. A. Jose et al [19] discussed accelerating the retinal image enhancement procedure. They presented parallel implementation of histogram equalization. When histogram equalization results on CPU and GPU are compared, execution time on CPU is 0.1157 seconds and on GPU 0.0781 seconds. So, parallel implementation on GPU is faster.

CHAPTER 2

MATERIAL AND METHODS

The automatic diagnosis of hypertensive retinopathy is achieved by using various methods and algorithms together. Basically, the materials and methods that are used can be summarized as follows. Initially, appropriate retinal image databases are selected to apply the selected methods and algorithms. Then, retinal images that are taken from the databases are enhanced with some pre-processing techniques to get better segmentation of retinal blood vessels. Calculation of the AVR value, which is the basic parameter used in the diagnosis of hypertensive retinopathy, is a rather troublesome process. This calculation is done after various processes are applied in a sensitive manner such as extraction of region of interest, measuring blood vessel calibers and classification of blood vessels according to their own properties. In this study, the methods and algorithms that have been used are time-consuming and they should be reorganized to improve performance. To overcome this issue, extensive research about GPUs has been done.

In this chapter, materials, methods and algorithms which are supposed to be backbone of the study have been mentioned in detail.

2.1 Retinal Image Databases

2.1.1 DRIVE

Digital Retinal Images for Vessel Extraction (DRIVE) is publicly available retinal image database for the purpose of comparative evaluation of retinal vessel segmentation [20]. It includes 40 digital color fundus images which are about population having subjects ranging between 31 and 86 years. These images are grouped into two main sets as 20 for test images and 20 for training images. All images are taken Canon CR5 non mydriatic 3CCD camera at 45 field of view (FOV) [21]. Each image in this database is 565×584 pixels wide. There also exists manually segmentation of each image which are done by ophthalmologists and mask

of each images. In Figure 2.1, sample image from DRIVE database with its mask and manual segmentation is presented.

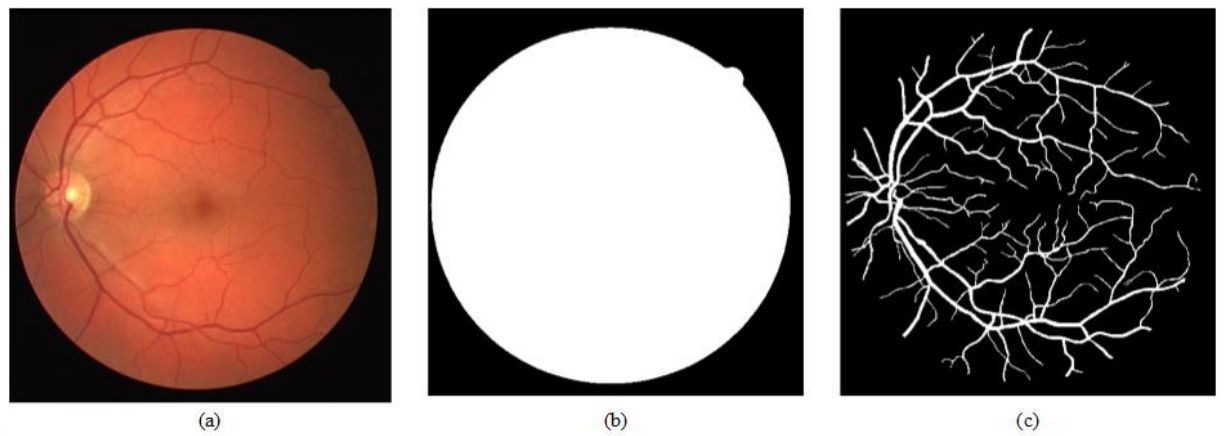


Figure 2.1 Sample from DRIVE database (a) The original image (b) The mask of an original image (c) Manual segmentation of blood vessels.

2.1.2 STARE

Structured Analysis of the Retina (STARE) [22] project is started in 1975 at the University of California, San Diego. Images are taken by TopCon TRV-50 fundus camera at 35 FOV and images are digitized to 605×700 pixels and 8 bits per color [21]. It contains 80 images for optic disc detection and 20 images for blood vessel segmentation with their hand labelled images. Images for blood vessel segmentation are manually segmented by two observers. The sample image and its two hand segmented images in Figure 2.2 are taken from database.

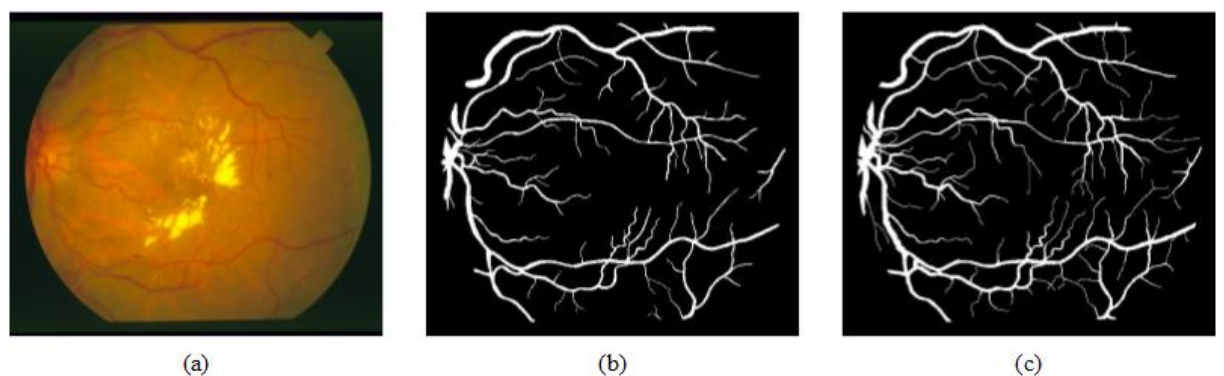


Figure 2.2 Sample from STARE database (a) The original image (b) Manual segmentation by first observer (c) Manual segmentation of blood vessels by second observer.

2.2 Retinal Image Pre-processing

Pre-processing step plays crucial role in segmenting the blood vessels of retina. This procedure aims to improve visual view to get better image for further analysis. It is important that retinal images must be well enhanced for highly precise diagnosis of different eye diseases. The most popular image enhancement methods have been explained in this section.

The first step of image pre-processing is converting input retinal image from RGB to grayscale. Since all subsequent operations are performed on this grayscale image, the success of this step affects the success of further steps. Retinal image is a RGB color image. RGB images consist of three image channels. In each pixel, color information is stored in these channels such that red (R), green (G), and blue (B). Grayscale images consist of different shades of gray. These types of images are also known as black and white images because color that they are stored, is varying from darkest black to lightest white [23]. There are several ways to obtain grayscale images from RGB. With different weight values of R, G, B channels, grayscale images can be obtained at diverse levels of gray. This process may vary depending on what work is performed. For the diagnosis of HR, it is important that the retinal blood vessels are distinct and can be distinguished from the background. When grayscale conversion is calculated by multiplying with different coefficient values for R, G, B, it is seen that the most suitable result is taken on the green channel because of retinal blood vessels give highest contrast in this channel [20].

After the image is converted into the grayscale image format, the next pre-processing step is applied. This step is called image enhancement. The most popular image enhancement method is histogram equalization [24]. Histogram equalization is a method to improve overall contrast of input image. It is a simple and efficient way to adjust contrast of image. It uses probability density function of the image to equalize the gray values level of it [25]. The probability density function of an image is given by equations in 2.1 and 2.1a, where p_n denotes the normalized histogram of given image X_k .

$$p_n(X_k) = \frac{\text{\# of pixels with intensity } n}{\text{total number of pixels}} \quad n = 0, 1, \dots, L - 1 \quad (2.1)$$

$$\sum_{n=0}^{L-1} p_n(X_k) = 1 \text{ and } 0 \leq X_k \leq 1 \quad (2.1a)$$

To obtain a histogram equalization function cumulative distribution function S_k of X_k is calculated by using the equation 2.2,

$$S_k = T(X_k) = \sum_{j=0}^k p_n(X_k) = \sum_{j=0}^k \frac{n_j}{n}$$

$$\text{where } k = 0, 1, \dots, L - 1 \text{ and } T(X_{L-1}) = 1 \quad (2.2)$$

Histogram equalization is simply spreading out the cumulative distribution function. In Figure 2.3, results of applying the histogram equalization function to the whole image are illustrated.

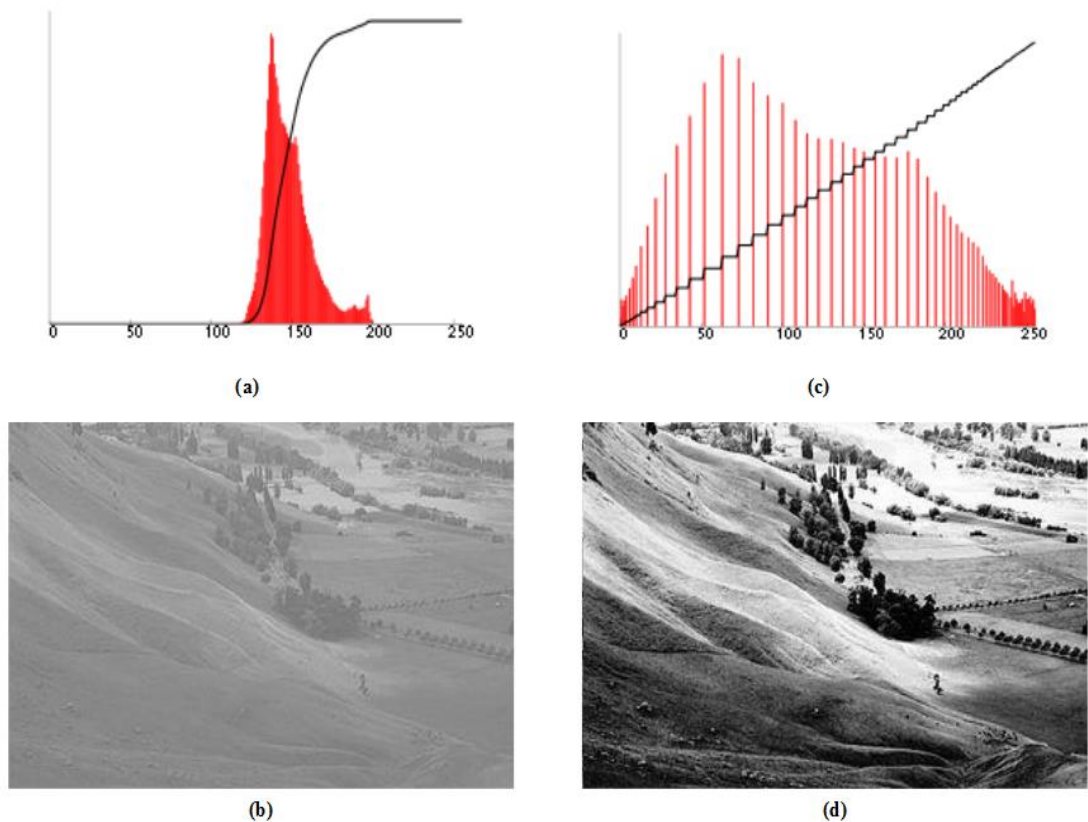


Figure 2.3 (a) Histogram of original image (b) Original image (c) Histogram of equalized image (d) Histogram equalized image [26].

When the histogram equalization works on the whole image, it is called global histogram equalization. Global histogram equalization produces different results depending on the characteristics of image [27]. If the distribution of pixel values is similar throughout the image, histogram equalization works well. Nevertheless, image can consists of mostly brighter or darker areas than the large part of the image. That's way the contrast in those areas is not enough enhanced by histogram equalization.

Retinal images are not uniformly enlightened and have contrast variability. Blood vessels should be brighter than background by enhancing image to get better result from blood vessel segmentation. To solve this, Contrast Limited Adaptive Histogram Equalization (CLAHE) can be applied to the retinal images. The CLAHE algorithm adaptively enhances image by limiting contrast unlike histogram equalization. The main idea behinds this algorithm, it optimizes the contrast enhancement by diving image into number of small tiles which are non-overlapping and applies global histogram equalization to each of these contextual regions. In the final process each tile is combined with the interpolation technique and whole image is reconstructed [28, 29].

2.3 Retinal Image Segmentation

Different objects in an image can be easily recognized by human brain. However, they can be diagnosed after quite complex operations with computer systems. In retinal images, distinguishing blood vessels from background is possible with number of image processing algorithms. Segmentation of blood vessels plays significant role to diagnose various eye diseases especially hypertensive retinopathy. Image filtering and thresholding are common methods to segment the image because of their ease of application. In this part of the thesis, common concepts and methods for segmentation step have been explained.

Filters are used in the preprocessing step as well as image segmentation. They make vessels more prominent for segmentation when applied to an enhanced image. Average filtering is used to reduce noise by smoothing images. It is simple and easy to implement. It works by replacing each pixel value in an image with the average

(mean) value of its neighbor pixels. So, the pixel which are different from its neighbors are eliminated by filtering process [30].

Retinal image processing is a major requirement for diagnosis of retinal disorders. Image segmentation is an important part of retinal image processing. It is a process of dividing or clustering the image into different regions corresponding objects. These regions have some common features like color, shape, intensity or texture. For retinal images, there are many objects to be accurately extracted. The main objects for diagnosing and treatment of hypertensive retinopathy are the blood vessel tree and the optic disc [31]. Therefore, these objects should be clearly separated from background. The blood vessel tree has a bright structure when compared to the dark background in the grayscale retinal image. It is aimed that the segmentation can be done properly by the pre-processing operations that are described in the previous section.

In this study, global thresholding method has been used to segment blood vessel tree because it is a proper method to separate bright and dark regions from each other. By the thresholding method, a binary image is obtained from the grayscale image by converting the pixel values below a certain threshold value to 0 and the others to 1. Thresholding is applied based on the idea presented in equation 2.3 where $b(x, y)$ is a binary version of grayscale image $g(x, y)$ at global threshold value T .

$$b(x, y) = \begin{cases} 1 & \text{if } g(x, y) > T \\ 0 & \text{otherwise} \end{cases} \quad (2.3)$$

In the retinal image thresholding, the binary image is obtained in such a way that the blood vessels are white (1) and the background is black (0). The threshold value parameter that is used in this step has a direct effect on the success of thresholding should be predetermined.

2.4 Extraction of Region of Interest

A region of interest (ROI) is an identified part of an image that to perform some image processing operations for a particular purpose. Finding region of interest in retinal images may vary according to which knowledge will be desired. Generalized

arteriolar narrowing, AVR, is significant sign for diagnosis of HR. The retinal blood vessels within the optic disc must be determined and classified as artery and vein. The AVR value is estimated from caliber of individual artery and vein in an area which is centered with optic disc [32]. Therefore, ROI is the optic disc for the investigation of HR. In this section, image processing methods and techniques that are used in determination of the location of the optic disk has been mentioned.

2.4.1 Mathematical Morphology

Mathematical morphology is a technique for extracting image components based on geometrical shapes. The goal of it in digital images is simplification of image data by preserving its shape and eliminating imperfections [33]. Identification of objects, extracting features of image are directly related with the shape, so mathematical morphology operators especially are used in image segmentation, object recognition, noise removal and image enhancement of images [34].

Different image processing operations can be used by combining different operators of mathematical morphology. In morphological operations, to probe the input image a shape which is called as structuring element is used. It is placed in all possible positions in the image and the corresponding pixel is compared with its neighboring pixels. When probing of an image with a structuring element, it fits, hits (intersects) and neither fits nor hits the image.

Morphological operators are basically introduced into various forms by using erosion and dilation. Erosion simply erodes the boundaries of region of foreground pixels whereas dilation enlarges the boundaries of foreground pixels. In the closing operation dilation and erosion are used consecutively to close small holes or small black points on the foreground pixels. In addition, opening is a dilation of erosion which removes small objects from the foreground of an image by replacing foreground pixel with background pixel. In Figure 2.4 example images about erosion and dilation are presented.

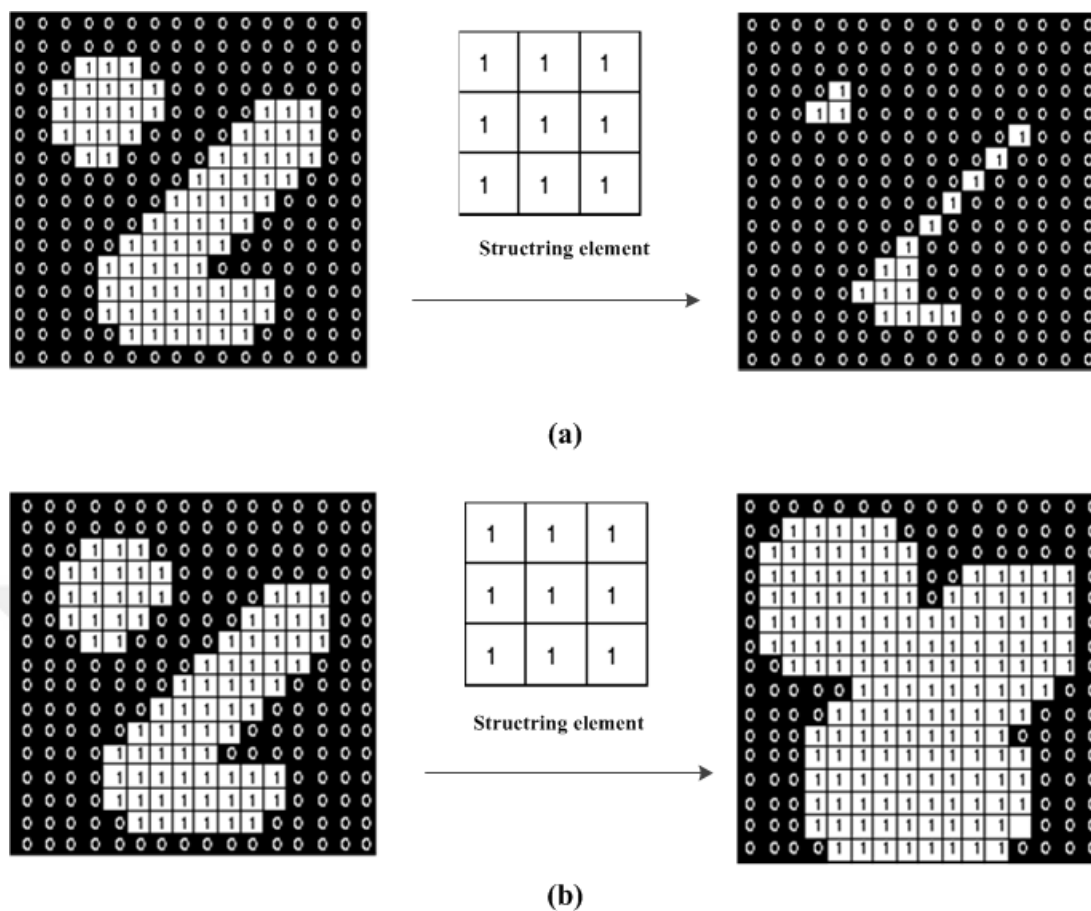


Figure 2.4 Morphological operators (a) Erosion (b) Dilation.

2.4.2 Canny Edge Detection

Edge detection is a set of mathematical methods to find sharp changes in digital image brightness. The set of points which brightness vary sharply are called as edges. When edge detector is applied to the image, it creates set of connected curves. These curves form the boundaries of objects within the images. Edge detection is mainly used in image processing, computer vision and especially features detection and extraction. There are different edge detection methods. Prewitt [35], Sobel [36] and Canny [37] are accepted as basic methods in the literature.

Sobel operator uses a pair of 3x3 convolution kernels which are perpendicular with each other. These kernels are designed to get maximum response from edges at vertical and horizontal position [38]. Each gradient component is obtained separately by applying kernels to input image and these components are combined to calculate

gradient magnitude according to the equations given in 2.4 and 2.4a where G_x, G_y are kernels to compute G which represents the magnitude.

$$|G| = |G_x| + |G_y| \quad (2.4)$$

$$G_x = \begin{bmatrix} -1 & 0 & +1 \\ -2 & 0 & +2 \\ -1 & 0 & +1 \end{bmatrix} \quad G_y = \begin{bmatrix} +1 & +2 & +1 \\ 0 & 0 & 0 \\ -1 & -2 & -1 \end{bmatrix} \quad (2.4a)$$

The main advantage of Sobel operator is simplicity of it. It provides approximation to the gradient magnitude and detects edges and their orientation. However, it is sensitive to noise and it can produce inaccurate edges.

Canny edge detection method works in a complex manner when it is compared with Sobel operator. In Canny, any noise in the image is reduced by Gaussian filter at first. After smoothing the image, for each pixel's edge gradient and direction is calculated. Then, pixels that are not considered to be part of an edge are removed. Finally, pixels gradient values are compared with the upper and lower threshold value, it is accepted or rejected as an edge [37]. Canny edge detection method is good at detection of only existent edges and finding localization of distance between detected edge pixels and real edge pixels. On the other hand, there are some disadvantages of Canny method. It is difficult to implement and time consuming.

2.4.3 Circular Hough Transform

There are many studies in the literature regarding the detection of optic disc [39, 40, 41]. When the methods that are used in these studies are grouped, it is seen that there are two main approaches; pixel-based and model-based. In the pixel-based approach, each pixel is evaluated one by one to determine whether it belongs to optic disc region or not. In the model-based approach, since one pixel is meaningful with pixels around of it, so pixels group is used to decide whether they are part of an optic disc region. In this work, pixel-based and model-based approaches are used together.

The Hough Transform is proposed to detect features of particular shapes in the image such as straight lines, circles [42]. To find optic disc in image with its edges that are

found by Canny Edge Detection method, firstly rounded shapes that are candidate to be an optic disc should be found. This task has been handled by using Circular Hough Transform. It is an extended version of standard Hough Transform for detection of circular objects in image [43]. If circle is wanted to be detected, points lying on the circle in three-dimensional space can be described by

$$(x - x_0)^2 + (y - y_0)^2 = r^2 \quad (2.5)$$

$$x = x_0 + r * \cos\theta \quad (2.5a)$$

$$y = y_0 + r * \sin\theta \quad (2.5b)$$

Equation 2.5 shows a circle with center (x_0, y_0) and the radius r . The circular shape determination using the Hough Transform can be summarized in general by the following steps [41].

1. Find the edges of an input image
2. Convert input image with edges found to binary
3. Set values for x_0 and y_0
4. Solve for the value of r satisfies Equation 2.5
5. Update the accumulator matrix (3D Hough Matrix) with the value of (x_0, y_0, r)
6. Increment values for x_0 and y_0 within the range of interest and go back step 3 until find candidate circles

2.5 Image Processing with MATLAB

MATLAB is a software environment for numerical computation. It is used in various branches of science like mathematics, engineering and electronics. MATLAB has more than 40 toolboxes and Image Processing Toolbox (IPT) is one of them for implementation and testing [44]. MATLAB R2014b has been used as the development environment for the studies that have been conducted within the scope of this thesis.

IPT is used in image analysis and assessment as well as feature extraction. It has all the necessary tools for image processing. Basically, image is composed of two-dimensional or three-dimensional matrix and there are four types of images which are grayscale, binary, color (RGB), indexed color. While implementation step of this thesis, functions of this toolbox have been frequently used. These can be listed as follows;

- Loading image functions: `imread`, `imshow`, `rgb2gray`,
- Image enhancement and thresholding functions: `imhist`, `histeq`, `graythresh`, `im2bw`
- Filtering functions: `imfilter`, `fspecial` (gaussian, average), `medfilt2`
- Morphological operations functions: `imclose`, `imopen`, `imerode`, `imdilate`
- Edge detection functions: `edge` (sobel and canny detectors)

2.6 Parallel Computing on GPUs with MATLAB

In medical image processing, the performance of the application is as much important as the output sensitivity and accuracy. In particular, a number of sophisticated algorithms running on high resolution images require slow processing because of the overhead required. The only way to achieve a faster result in the case the problem cannot be resolved without complex algorithms and various operations (convolution, filtering, matrix multiplication and so on) on large matrices but high precision is required is dividing the input data in smaller segments. Thus, the operation to be performed by simultaneously executing the same algorithm on each data set divided into smaller parts is completed in a shorter time. This technique is called “Data Parallelism”. Significant performance improvement is observed when data parallelism is applied in some image processing techniques [45, 46]. The working principle of data parallelism is illustrated in Figure 2.5.

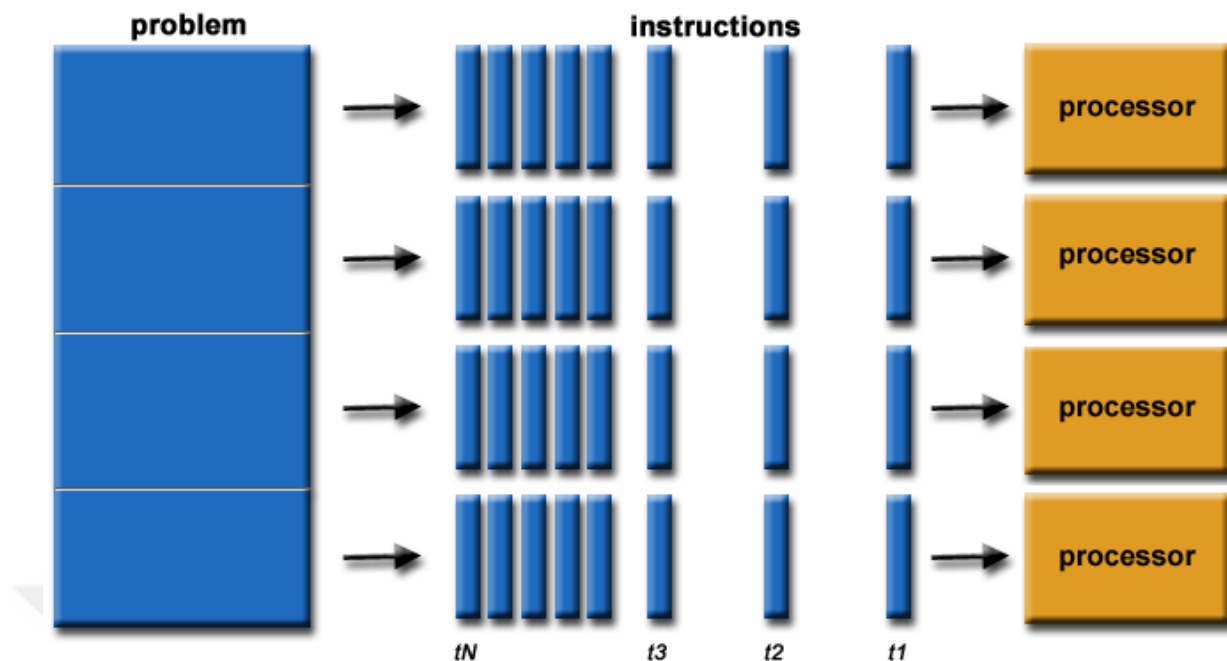


Figure 2.5 The working principle of data parallelism.

The improvements on processing technology allow researchers to use data parallelism on multi-core processors with slight software modifications. Especially, GPUs are practical and useful for parallel programming. With hundreds or even thousands of processor counts, GPUs are being used more and more in big data projects, in problems which are only resolved by applying complex algorithms such that optimization problems, in graphics rendering and particularly in image processing projects [47]. In Figure 2.6, hardware architectures of CPU and GPU are depicted.

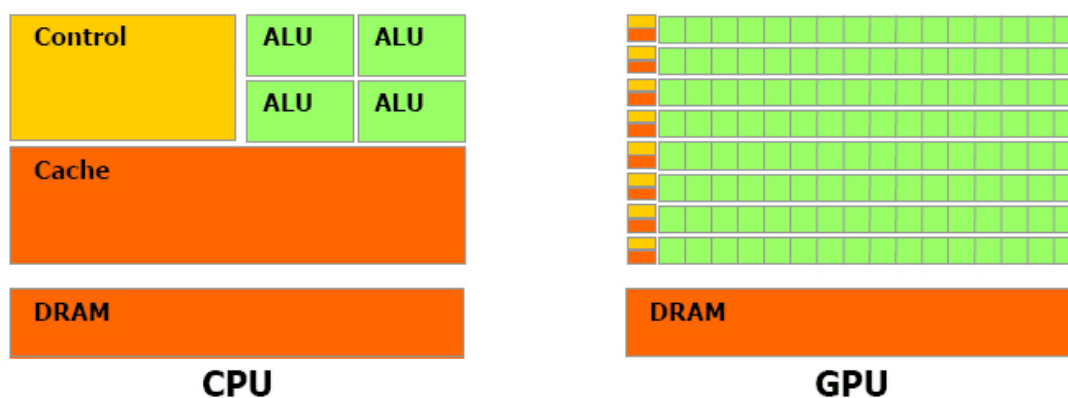


Figure 2.6 Hardware architectures of CPU and GPU.

GPUs are able to produce very fast results in matrix operations compared to CPUs. GPUs are very important for this study since retinal images are the basis of this work and images are treated as 2D matrix. Hence, image processing algorithms are applied on this 2D matrix. In the study conducted within the scope of the thesis, some of the image processing algorithms working on 2D retinal images were parallelized using GPUs. Parallelization was performed on the NVIDIA TESLA K20c and MATLAB R2014b was used as software development environment. With the help of MATLAB Parallel Computing Toolbox (PCT), image processing algorithms can be parallelized. Parallel programming on GPUs using MATLAB can be implemented in basically three different ways [48].

- Using GPU enabled built-in functions that are maintained by MATLAB PCT,
- Using "arrayfun" command on gpuArray.
- Using the MATLAB/CUDA run existing CUDA/C++ codes.

The choice made from three different methods does not affect performance directly. The difference between three methods is just about how to make parallelization. In this study, for image processing purposes MATLAB IPT is mainly used, therefore all codes from the scratch were implemented completely on MATLAB. In order to preserve the code unity, first parallelization method was chosen and implemented. With the help of GPU enabled built-in functions provided by MATLAB PCT, the image processing algorithms described in the following sections can be easily parallelized.

2.6.1 GPU-enabled built-in Image Processing Functions

To process an image on the GPU, firstly, the image data must be copied from the CPU memory to the GPU memory over PCI bus. In MATLAB, the image data on the GPU is accessed via the gpuArray object. When new gpuArray object created from image data, the data type of gpuArray is same as image data type. After all executions on GPU is completed, result object is copied back to CPU memory with gather function. However, copying over the PCI bus is a slow for this reason unnecessary copying should be avoided. To manipulate image data on GPU memory,

MATLAB provides list of GPU-enabled functions. IPT provides useful GPU-enabled functions and time performance can be measured within the tic() toc() blocks. In the Figure 2.7, sample code fragment is given.

```
imGpu = gpuArray (im);  
tStart = tic();  
sobelFilter = fspecial ('sobel');  
filteredImGpu = imfilter(imGpu, sobelFilter);  
tEnd = toc(tStart);
```

Figure 2.7 GPU-enabled imfilter function.

2.6.2 arrayfun on gpuArray

Calling existing functions through the arrayfun function allows manipulating GPU arrays directly from MATLAB. When comparing the GPU-enabled built-in functions and arrayfun function for large functions to be run on GPU, writing own functions and calling through the arrayfun is faster [49].

2.6.3 CUDA Kernel

It is possible to call our own CUDA-implemented algorithms via MATLAB with the CUDAKernel object. At the same time, the use of global memory and shared memory can be managed in this way. To start a CUDA kernel function, the CUDAKernel object is created by calling the parallel.gpu.CUDAKernel constructor. This constructor takes three inputs. First one is the path .ptx contains kernel code, second one is a .cu interface, and the third one is desired kernel. In addition, when CUDAKernel object is constructed, ThreadBlockSize, GridSize, and SharedMemorySize properties must be specified [48] and examples can be seen in Figure 2.8.

```
% myFilters.cu contains kernel like myFilter1, myFilter2, myFilter3
gpuFilter = parallel.gpu.CUDAKernel('myFilters.ptx', 'myFilters.cu', 'myFilter1');

%Declaration of desired myFilter1 kernel function
__global__ void myFilter1(const float *imIn, float *imOut, float parameter)

%Properties setting
gpuFilter1.ThreadBlockSize=[32 8 1]; % 32*8 threads
gpuFilter1.GridSize=[96 384 1]; % 96*384 blocks
gpuFilter1.SharedMemorySize=4*32*8; % 4*32*8=1024 bytes per block
```

Figure 2.8 CUDA Kernel.



CHAPTER 3

IMPLEMENTATION

In this chapter, the implementations of the methods described in Chapter 2 using MATLAB on both CPU and GPU have been explained. Basically, the procedures for the diagnosis of hypertensive retinopathy have been carried out in 5 basic steps. First of all, the quality of retina image from the DRIVE or STARE database has been improved using image enhancement algorithms. For second step, enhanced retina image has been segmented to examine the retinal blood vessel in region of interest. Afterwards, region of interest in retinal images has been determined by detecting optic disc location. Retinal blood vessels have been classified into arteries and veins according to their characteristics such as vessel diameter and color. Finally, according to the classified vessels AVR value has been computed and diagnosis of hypertensive retinopathy has been done. On the other hand, the time-consuming parts of this implementation on the CPU have been accelerated using the GPU and the performance of the application has been increased. The operations performed in this chapter are explained in detail and the resulting images are shared.

3.1 Implementation Architecture

The developments that have been used in this thesis have been implemented by using MATLAB, which provides a great deal in terms of image processing methods and techniques. Both the functions that MATLAB IPT provides and the algorithms we have implemented have been used in the developments. In the thesis, an overview of the method that has been proposed for the diagnosis of hypertensive retinopathy has been shown in Figure 3.1.

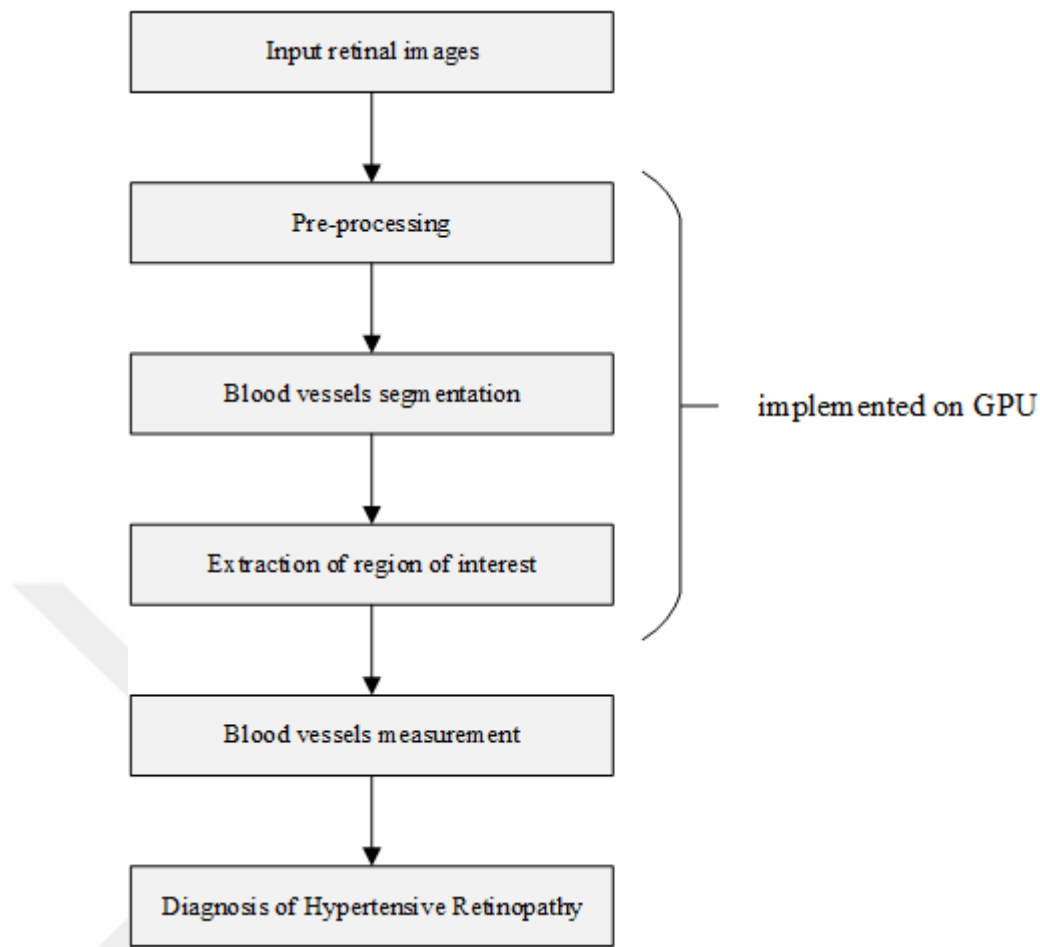


Figure 3.1 Steps of the proposed method.

In order to obtain high performance in the diagnosis of hypertensive retinopathy, which is basically composed of 5 steps, pre-processing, blood vessels segmentation and extraction of regions of interest have been accelerated with GPUs. To take advantage of the CUDA GPU computing, MATLAB has been preferred through Parallel Computing Toolbox because it can be implemented more easily and faster than C or any programming language. In the previous chapter, it is mentioned that there are several ways to use the GPU directly from MATLAB. GPU-enabled functions in different toolboxes have been preferred for implementation

The performance of the GPU depends on the resolution of the input image and on the CUDA device properties. When good results are obtained with better GPUs, certain steps of the implemented method may not achieve a significant difference from GPU

run times and CPU run times when the GPU features are not enough good. The CUDA device properties have been shown in Figure 3.2.

```
>> gpuDevice

ans =

  CUDADevice with properties:

      Name: 'Tesla K20c'
      Index: 1
  ComputeCapability: '3.5'
      SupportsDouble: 1
      DriverVersion: 8
      ToolkitVersion: 6
  MaxThreadsPerBlock: 1024
  MaxShmemPerBlock: 49152
  MaxThreadBlockSize: [1024 1024 64]
      MaxGridSize: [2.1475e+09 65535 65535]
      SIMDWidth: 32
      TotalMemory: 4.9658e+09
      AvailableMemory: 4.8686e+09
  MultiprocessorCount: 13
      ClockRateKHz: 705500
      ComputeMode: 'Default'
  GPUOverlapsTransfers: 1
  KernelExecutionTimeout: 0
      CanMapHostMemory: 1
      DeviceSupported: 1
      DeviceSelected: 1
```

Figure 3.2 CUDA device properties.

3.2 Pre-processing

In the retinal image, a number of pre-processing techniques are required to distinguish blood vessels from other parts of the retina. This also affects the success of the segmentation. Basically, the pre-processing step consists of two main steps

which are grayscale transformation and histogram equalization. The flowchart of this step is presented in the Figure 3.3.

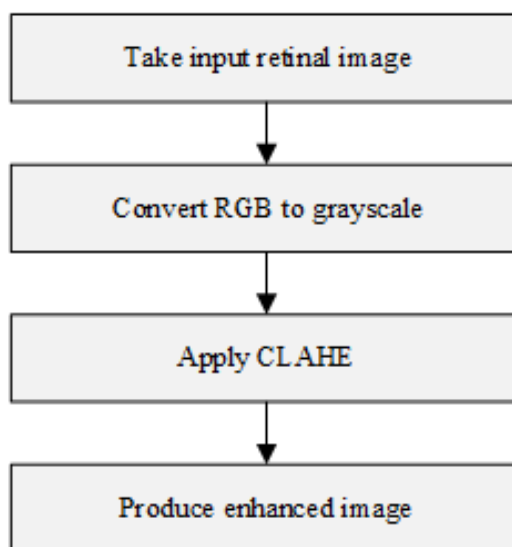


Figure 3.3 Pre-processing steps.

The input of pre-processing step is the retina image that is a RGB image. Firstly, red, green and blue channels of RGB image have been extracted separately. The obtained channel extraction results are shown in Figure 3.4.

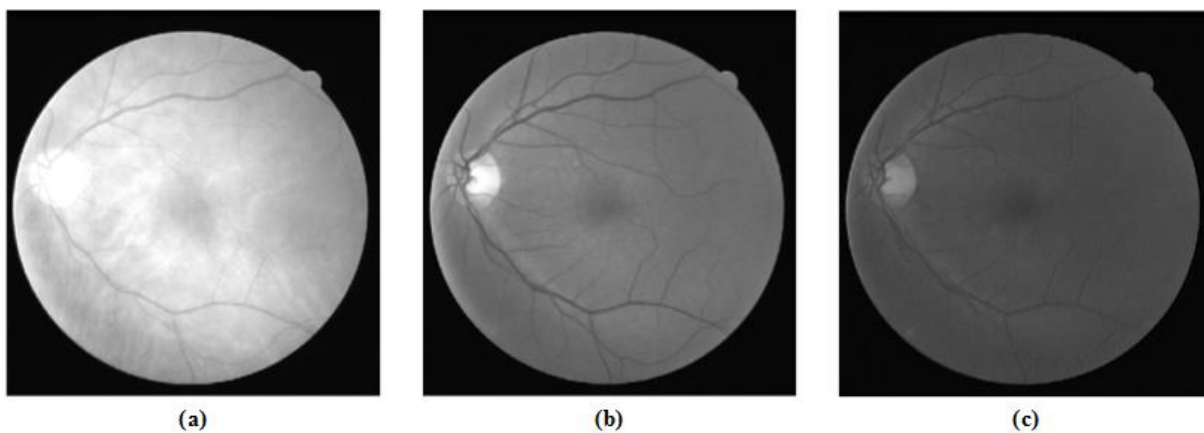


Figure 3.4 (a) Red channel (b) Green channel (c) Blue channel.

As mentioned in Chapter 2, there are different ways to obtain grayscale image from RGB image, in this work equations are shown some equations have been tried in turn and they have been given as follows:

$$I = (I_r + I_g + I_b)/3 \quad (3.1)$$

$$I = 0.21 * I_r + 0.72 * I_g + 0.07 * I_b \quad (3.2)$$

$$I = I_g \quad (3.3)$$

By using (3.1), the gray level image has been obtained by taking the average of all the color channels. Afterwards, (3.2) has been tried to increase contrast between blood vessel and background. Luminosity is calculated by heavily weighted G value. And then, when (3.3) has been tried, using the green channel it has been seen that the contrast between the blood vessels and the background reaches maximum value.

The input image has also been converted to a grayscale image to provide better results and to compare the resulting images. The comparison for grayscale and green channel of image is given in Figure 3.5. According to this comparison, it has been understood that the best result has been taken with the green channel of image.

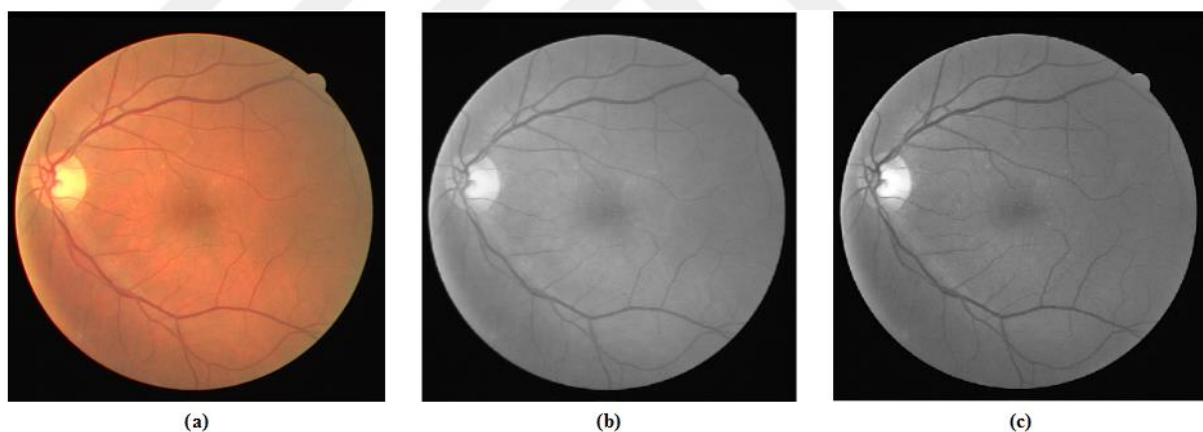


Figure 3.5 Comparison of grayscale and green channel (a) Original image (b) Grayscale image (c) Green channel image.

Another enhancement on the retinal image has been done by increasing the intensity of blood vessels. For this operation, the global histogram equalization and CLAHE have been used which has been performed green channel. In Figure 3.6, comparison of global histogram equalization and CLAHE on the green channel image has been illustrated and it has been figured out that CLAHE works well for image enhancement as against global histogram equalization.

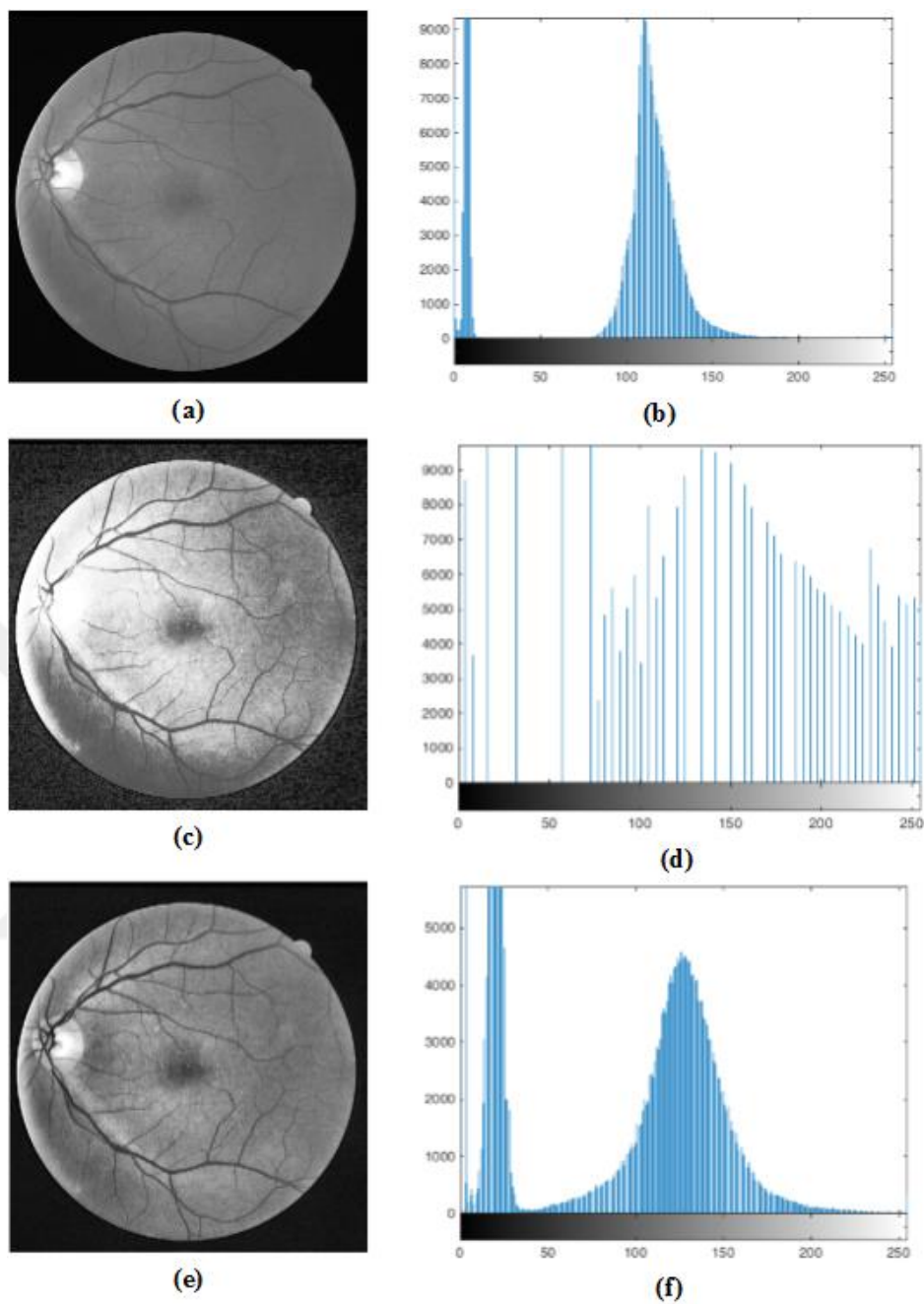


Figure 3.6 Comparison of Global HE and CLAHE (a) Green channel (b) Histogram of green channel (c) Global HE is applied (d) Histogram of Global HE (e) CLAHE is applied (f) Histogram of CLAHE.

In addition, converting image to double precision and taking green component of image have been implemented with the `gpuArray` of MATLAB PCT. With this way, parts of this implementation have been done on GPU.

3.3 Blood Vessel Segmentation

For diagnosis HR, the next step is blood vessel segmentation. The input image of this step is enhanced retinal image whose quality has been improved with pre-processing methods. In the study, different segmentation algorithms have been applied which have been summarized in flowchart that is illustrated in Figure 3.7.

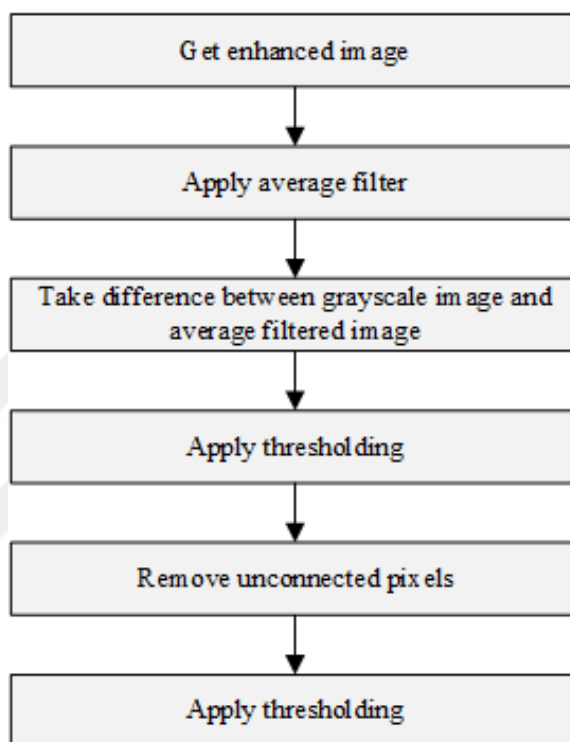


Figure 3.7 Blood vessel segmentation steps.

By applying average (mean) filter to the one copy of the input image, a blurred retina image has been obtained. This filtered image has been subtracted from original input image to isolate blood vessels from background of the retina. In other words, lines of the blood vessel in the image have been become more distinctive and apparent. With this way, it has been aimed to increase success of thresholding. Before applying filter, kernel matrix has been decided. To determine the best kernel matrix, steps in the following algorithm have been run.

1. Increase the size of the kernel matrix.
2. Apply average filter.

3. Extract average filtered image from original image.
4. Have the lines in the resulting image become clearer? If yes, go to step 1. If no, finish and use the size of the kernel matrix that applied last.

Accordingly, the appropriate size of the kernel matrix has been used. The size of the matrix can be reduced for higher success in lower resolution images, can be increased in higher resolution images. Average filtering has been applied on the retinal images in the DRIVE database by selecting kernel matrix in such manner. As a result of these trials, it has been observed that kernel matrices giving the best results are 9x9 and 11x11. Also, the implementation of average filtering has been done on GPU to accelerate processes.

In Figure 3.8, result images for background exclusion have been illustrated. This result has been obtained with subtraction of average filtered image from the input image.

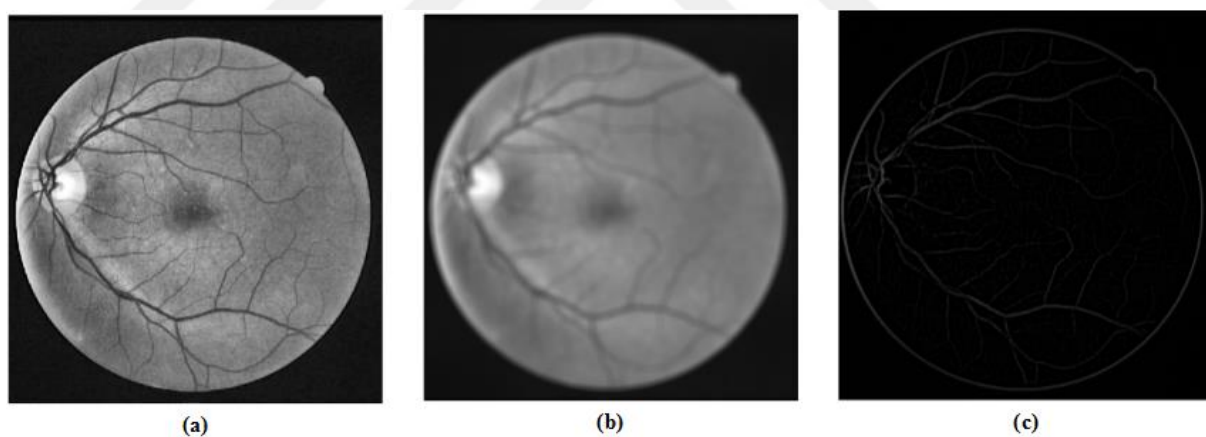


Figure 3.8 Retinal image background exclusion (a) Input image (b) Average filtered image (c) Background excluded image.

After this process, to segment retinal blood vessels thresholding method has been applied with a certain threshold value. The success of the thresholding method varies considerably according to the chosen correct threshold value. Retinal images may be depicted on different conditions, so manual determination of the threshold value may give satisfactory results for some images image, but for some images it may not give

the correct thresholding result. That's way; the threshold value must be specified for each image by automatically. There are various methods and techniques for automatically selecting the threshold value according to the properties of the input image.

In this study, different methods for determination of threshold value have been carried out to get best threshold value and their results have been compared. At first, thresholding has been applied to the input image with a threshold value which has been obtained by using Otsu's method. The threshold value has been computed with the help of "graythresh function" which is provided by MATLAB have been used. This function uses Otsu's method, which chooses the threshold to minimize the variance of the black and white pixels [50].

To compare results, another threshold value has been obtained by using iterative technique for choosing a threshold which was developed by Ridler and Calvard [51]. In this iterative technique, input image is divided into foreground and background by taking an initial threshold, then averages of the pixels at or below the threshold and pixels above are computed. The averages of those two values are computed, the threshold is incremented and the process is repeated until the threshold is larger than the composite average.

When the thresholding has been applied with the two different threshold values, there are some unconnected pixels in the image. These unconnected pixels that are below the 10 pixels have been removed and the thresholding process has been concluded. In Figure 3.9, the thresholding outcomes have been pictured. The closest thresholding result to hand labelled retina image by human observer from DRIVE database has been obtained with Ridler and Calvard iterative thresholding method. So, implementation has been continued by choosing this method.

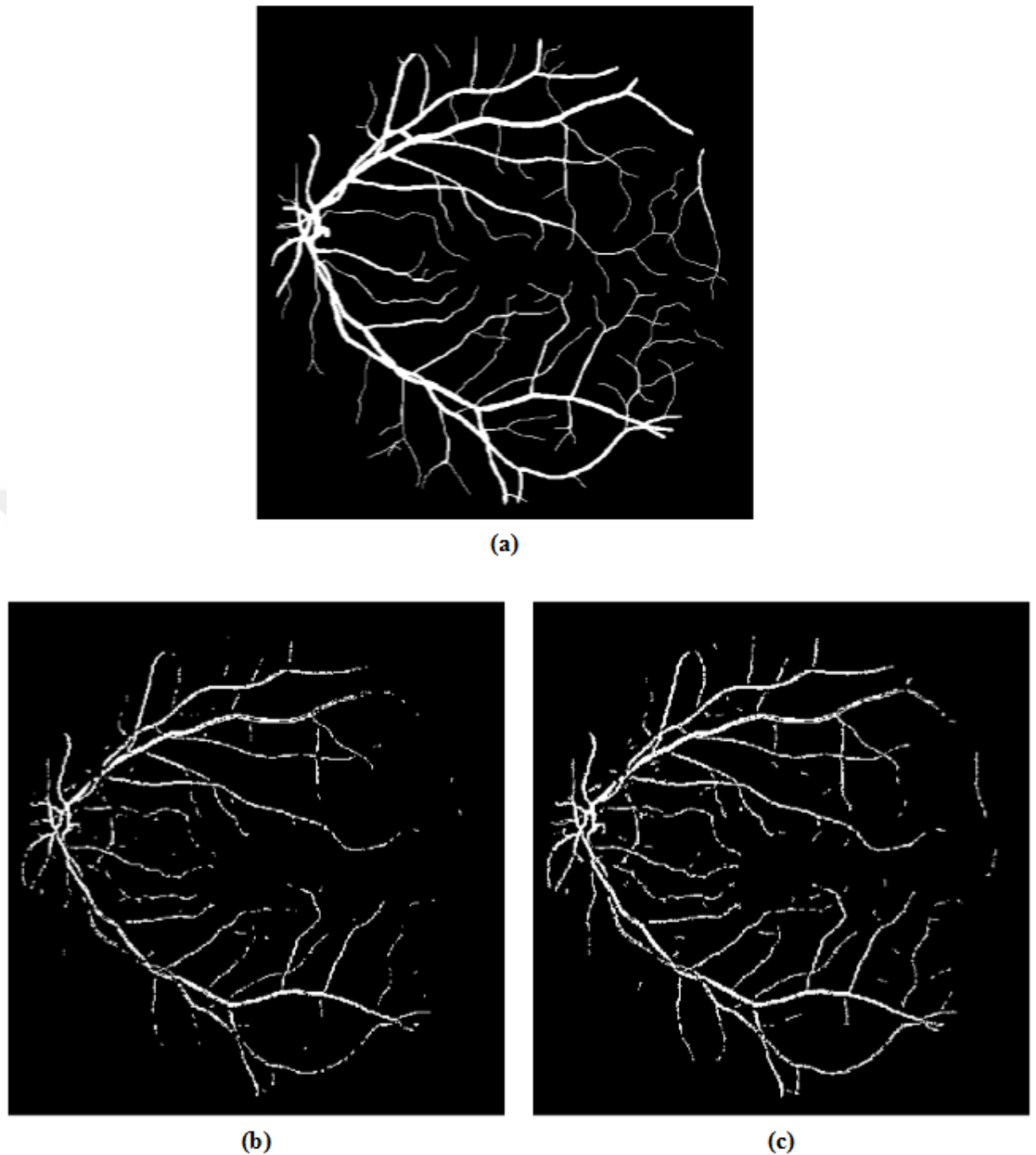


Figure 3.9 Segmentation results (a) DRIVE database hand-labelled segmentation (b) Segmentation with Otsu's method (c) Segmentation with iterative thresholding method.

3.4 Finding Region of Interest

The region of interest in retinal images which are used to examine HR is optic disc. For this reason, the detection of location of the optic disc is of major importance to solve this step. Within the scope of this thesis, to identify the location of the optic

disc means extracting region of interest, steps of implementation which have been shown in Figure 3.10 have applied respectively.

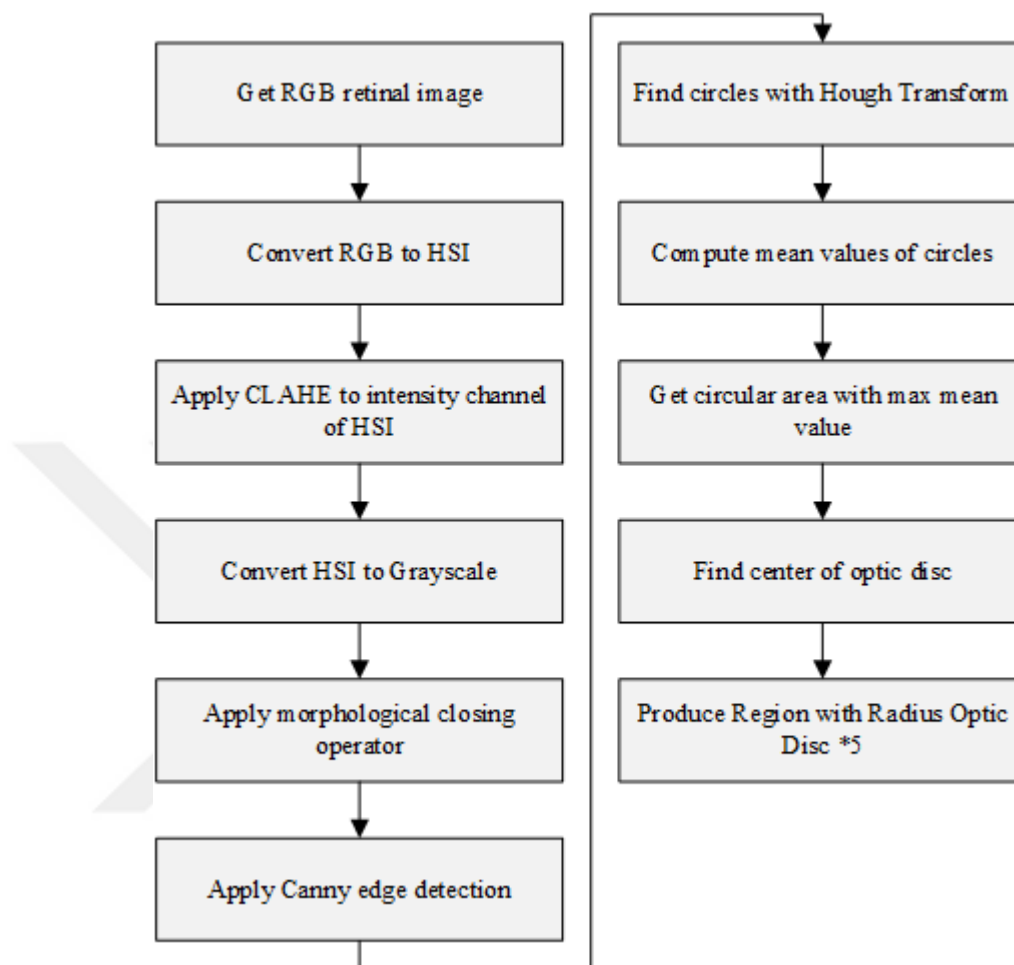


Figure 3.10 Extraction of ROI.

Optic disc has mainly round shape and region of it is considered to be the brightest area in the whole retina [52]. The light intensity in retinal images is mostly inhomogeneous. Since the distribution of light intensity is taken as a reference to identify the location of optic disc, the distribution in this channel must be homogenized. Input of this step is RGB retinal image, because light intensity component should be equalized. Human eye perceives color with simple three parameters which are hue, saturation and intensity. To make description of this process Hue Saturation Intensity (HSI) color model is commonly used. The hue is used to describe an actual color i.e., red, green or orange. For enhancement of images hue value should remain unmodified, saturation and intensity component should be

changed. While saturation describes the intensity of color, intensity is related with intensity of the light [53]. To equalize light intensity, RGB input image has been converted into HSI color space. To conversion from RGB to HSI equations which have been illustrated in (3.4), (3.5), (3.6) have been used. To enhance light intensity, CLAHE has been applied to the Intensity channel of HSI image. Then enhanced HSI format image again has been converted into RGB format by using equations that are shown in (3.7), (3.8), (3.9) [54].

Equations of conversion from RGB to HSI,

$$I = \frac{1}{3} (R + G + B) \quad (3.4)$$

$$H = \begin{cases} \theta & \text{if } B \leq G \\ 1 & \text{if } B > G \end{cases}, \text{ where } \theta = \cos^{-1} \left[\frac{\{(R-G)+(R-B)\}/2}{\sqrt{(R-G)^2+(R-G)(R+G)}} \right] \quad (3.5)$$

$$S = 1 - \frac{3}{(R+G+B)} [\min(R, G, B)] \quad (3.6)$$

Equations of conversion from HIS to RGB which depends on H sectors

$$RG \text{ sector: } 0^\circ \leq H \leq 120^\circ \quad \begin{cases} B = I (1 - S) \\ R = I \left[1 + \frac{S \cos H}{\cos(60^\circ - H)} \right] \\ G = 3I - (R + B) \end{cases} \quad (3.7)$$

$$GB \text{ sector: } 120^\circ \leq H \leq 240^\circ \quad \begin{cases} H = H - 120^\circ \\ R = I (1 - S) \\ G = I \left[1 + \frac{S \cos H}{\cos(60^\circ - H)} \right] \\ B = 3I - (R + B) \end{cases} \quad (3.8)$$

$$BR \text{ sector: } 240^\circ \leq H \leq 360^\circ \quad \begin{cases} H = H - 240^\circ \\ G = I (1 - S) \\ B = I \left[1 + \frac{S \cos H}{\cos(60^\circ - H)} \right] \\ R = 3I - (R + B) \end{cases} \quad (3.9)$$

After light equalization operation has been completed, the new enhanced image in RGB color space has been transformed into the grayscale format to remove blood

vessels from the grayscale retinal image. This process has been performed by using morphological closing operator. Closing has been applied with a disk-shaped structuring element to preserve the circular nature of optic disc. It has been specified with a radius of 10 pixels so that the largest gap gets filled. With the help of `imclose` function which is provided by MATLAB, the lines which are originated from blood vessels have been removed and only circular areas of image have been brought to the foreground. Morphological operations have been done on GPU and sample code fragment has been given in Figure 3.11 and the obtained image has been shown in Figure 3.12.

```
%% Read retina image.
originalImage = imread('retina.png');

%% Equalize light intensity of image
enhancedImage = {...}

%% Create a disk-shaped structuring element.
se = strel('disk',10);

%% Convert array to gpuArray.
gpuArrayImage = gpuArray(enhancedImage)

%% Perform a morphological close operation on the image on a GPU.
closedImage = imclose(gpuArrayImage,se);
```

Figure 3.11 Morphological closing implementation on GPU.

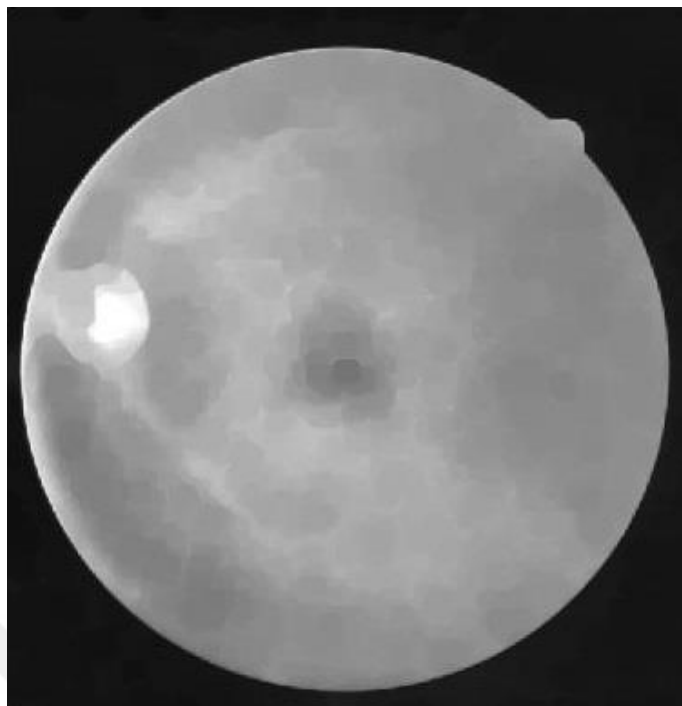


Figure 3.12 The result of morphological closing operation.

It is aimed to identify the edges of the circular areas in the morphologically closed image. To achieve this, Sobel and Canny edge detection methods have been used and results have been compared with each other. According to this comparison, Canny method gave the best result with the 0.1 threshold value. In Figure 3.13 the detected edges of image can be seen.

After that, Circular Hough Transform has been applied to the image where the edges have been found to localize all candidate optic disc patterns. The retina images in the DRIVE database have been manually analyzed to identify radius range of circles to be detected. As a result of this analysis, all circular shapes those radii are in the interval of 17-55 pixels have been scanned and these have been marked as candidate optical areas. The circular shapes that are found are illustrated in Figure 3.14.

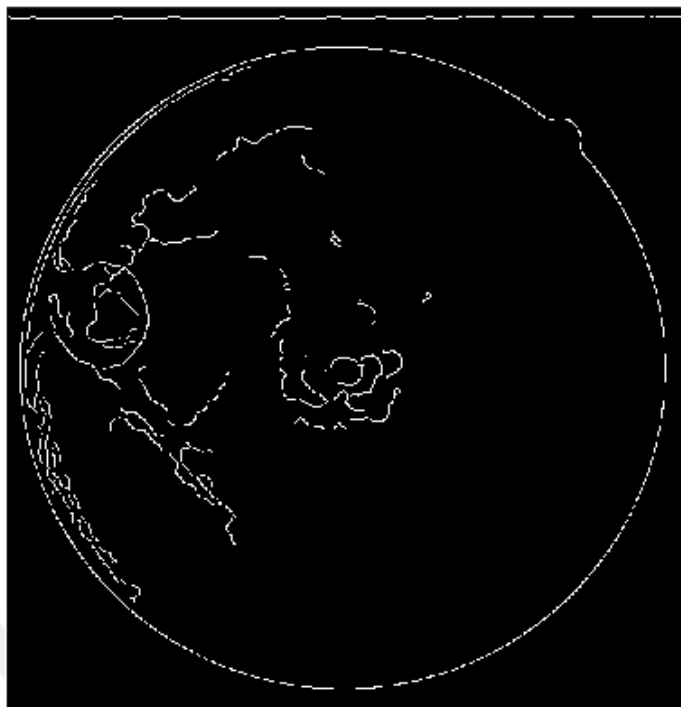


Figure 3.13 The detected edges with Canny's method.

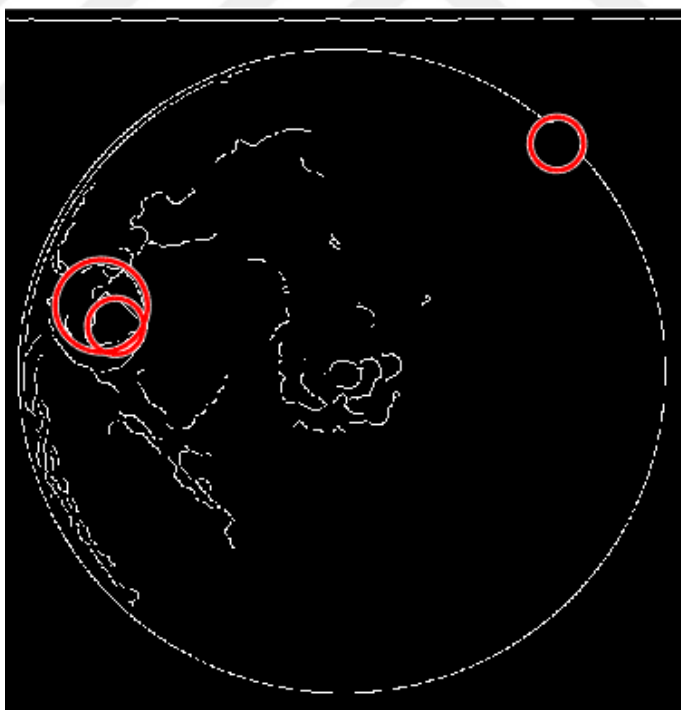


Figure 3.14 The detected circular shapes with Circular Hough Transform.

Finally, the mean values have been calculated for all the circular areas that are obtained using the Circular Hough Transformation. The area with the greatest mean

value and the largest radius has been selected as the optic disc. In this way, the location information of the optic disc has been determined as shown in Figure 3.15.

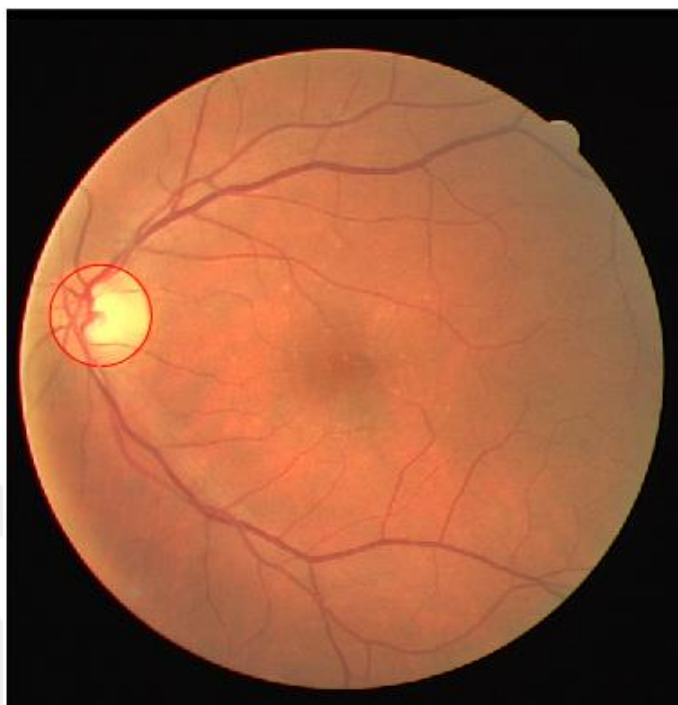


Figure 3.15 The detected optic disc.

As mentioned before, classifying blood vessels, measuring caliber of them and calculating AVR have importance to diagnose hypertensive retinopathy. AVR is calculated from the values of arteriolar and venular calibers inside the region of interest (ROI). ROI is an area centered on the optic disc and half disc to one disc diameter from the optic disc margin [55]. With the knowledge about optic disc found in previous section and the ROI, this specific area has been determined. The details of the code implemented in the scope of this work have been given in the Figure 3.16 as a pseudocode.

```

1  Take RGB retinal image as an input;
2  Convert input image to HSI format;
3  Apply CLAHE to Intensity channel of HSI;
4  Convert HSI image to RGB image;
5  Convert RGB image to grayscale format;
6  Apply morphological closing;
7  Find edges;
8  Find circles;
9
10 WHILE number of circle found equals 0
11     Apply morphological closing;
12     Find circles;
13 ENDWHILE;
14
15 FOR number of circle found
16     Calculate mean value of circular area for each circle
17 ENDFOR
18
19 Get circular area with max mean value;

```

Figure 3.16 The pseudocode for finding region of interest.

3.5 Measurement of the Diameter of Blood Vessels and AVR

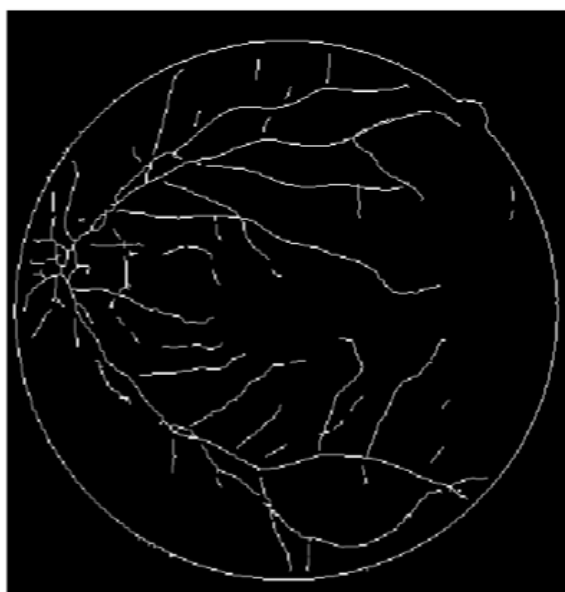
AVR value is a necessary measurement for diagnosis of hypertensive retinopathy. To calculate this value, the blood vessels in the region of interest must be classified as artery and vein. This classification can be done by examining the major vessels which are located at a circular region around the optic disc. These major vessels directly come from the optic disc. Ophthalmologists usually distinguish these major vessels into arteries and veins by their color and thickness. In a study main arteries and veins that are running parallel to each other are used to calculation of AVR and classification of blood vessels are done according to color components of them [56]. In another study automated method for classification of blood vessels is proposed on the basis color feature in RGB, HSL, LAB color spaces [57]. However it is not enough to separate vessels from each other only considering color feature. Thickness of blood vessels is a feature that distinguishes the vessels from each other.

In this thesis, blood vessel classification was done by using measured diameter feature of vessel. First of all, all major vessels were found by indexing in the predetermined region of interest and the thickness information for each indexed vessel was then measured. As a first step in measuring vessel diameter, the edges of the segmented retinal image were determined that was done with the help of Canny

Edge Detection method. The index information of the edges of the vessels was kept in a matrix. In addition, the morphological thinning was applied to the original segmented image to provide centerline of the vessels and the index information of these centerlines was also kept in a separate matrix. In Figure 3.17, centerline image and edge image can be seen. Simply, calculating diameter of the vessel was done by finding distances between point which is taken from the centerline matrix and the nearest edge points that are taken from edge matrix.



(a)



(b)

Figure 3.17 (a) Image with vessels edge points (b) Image with vessels centerline points.

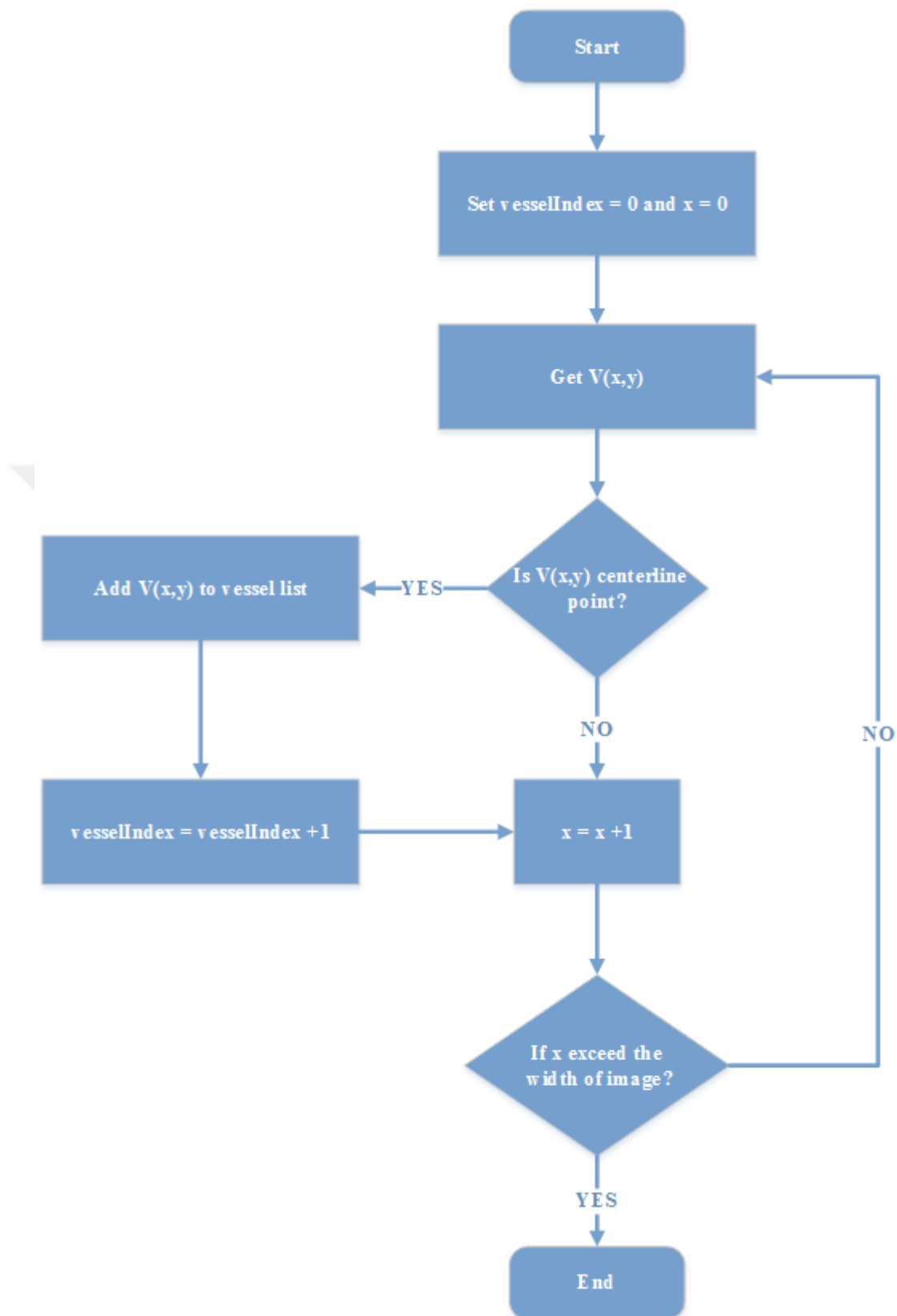


Figure 3.18 Flow diagram of discovering vessels around the center of optic disc.

It should be mentioned how the major vessels around the optical disk are detected. The flow diagram of discovering different vessels around the optic disc were shown in Figure 3.18. The finding vessels were achieved by shifting the y value optic disc center $O(x,y)$ up and down by the optic disc radius r . First, the y value was taken as $y-r$ to scan upper part of the image and x value was initialized from 0. The value of each (x,y) pair was compared with the corresponding index in the centerline image. If the index value was equal to 1 (white pixel) then this point was chosen as a vessel centerline point. And this process was continued incrementing the x value by 1 until it reaches the region of interest boundaries. With this approach, all different major vessels in the upper part of optic disc were detected. The same process was reproduced by increasing the y value by r to detect major vessels in the lower part of the optic disc. These detected vessels were kept in a list to calculate their thicknesses.

The next process was applied to find nearest edge points to the centerline points. Firstly, the centerline point of the first of the vessels was taken. Formulas that are shown in equations (3.10) and (3.11) were used to find the index of the nearest edge pixel using target centerline pixel $C(x,y)$. The value of R was incremented one by one starting from 1 until the edge pixel was found while the θ value was 0 degrees. For each R value x_1 and y_1 values were calculated and the value of edge pixel $E(x_1,y_1)$ was checked if it was 1 or not. If this value was equal to 1, it meant that edge pixel was found.

$$x_1 = x + R * \cos(\theta) \quad (3.10)$$

$$y_1 = y + R * \sin(\theta) \quad (3.11)$$

After detection the edge pixel, the distance between $C(x,y)$ and $E(x_1,y_1)$ was found using Euclidean distance. The equation was indicated in (3.12).

$$d = \sqrt{(x_1 - x)^2 + (y_1 - y)^2} \quad (3.12)$$

It was continued to calculate distance between centerline and edge by increasing the θ value. The shortest of these measured distances was taken and it was multiplied by 2 to calculate thickness. This measurement procedure was illustrated in Figure 3.19. The same procedure was repeated for all vessel centerline points that were found before. In this way, the thicknesses of all major vessels in the region of interest were calculated.

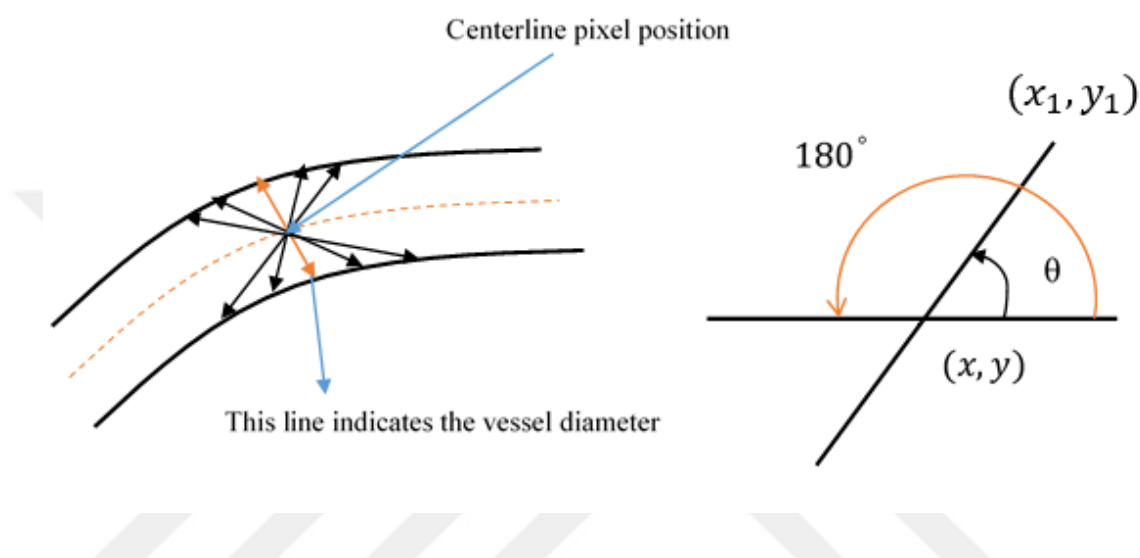


Figure 3.19 Measurement of vessel diameter.

Figure 3.20 shows the flow diagram of the algorithm that was applied to calculate thicknesses of vessels.

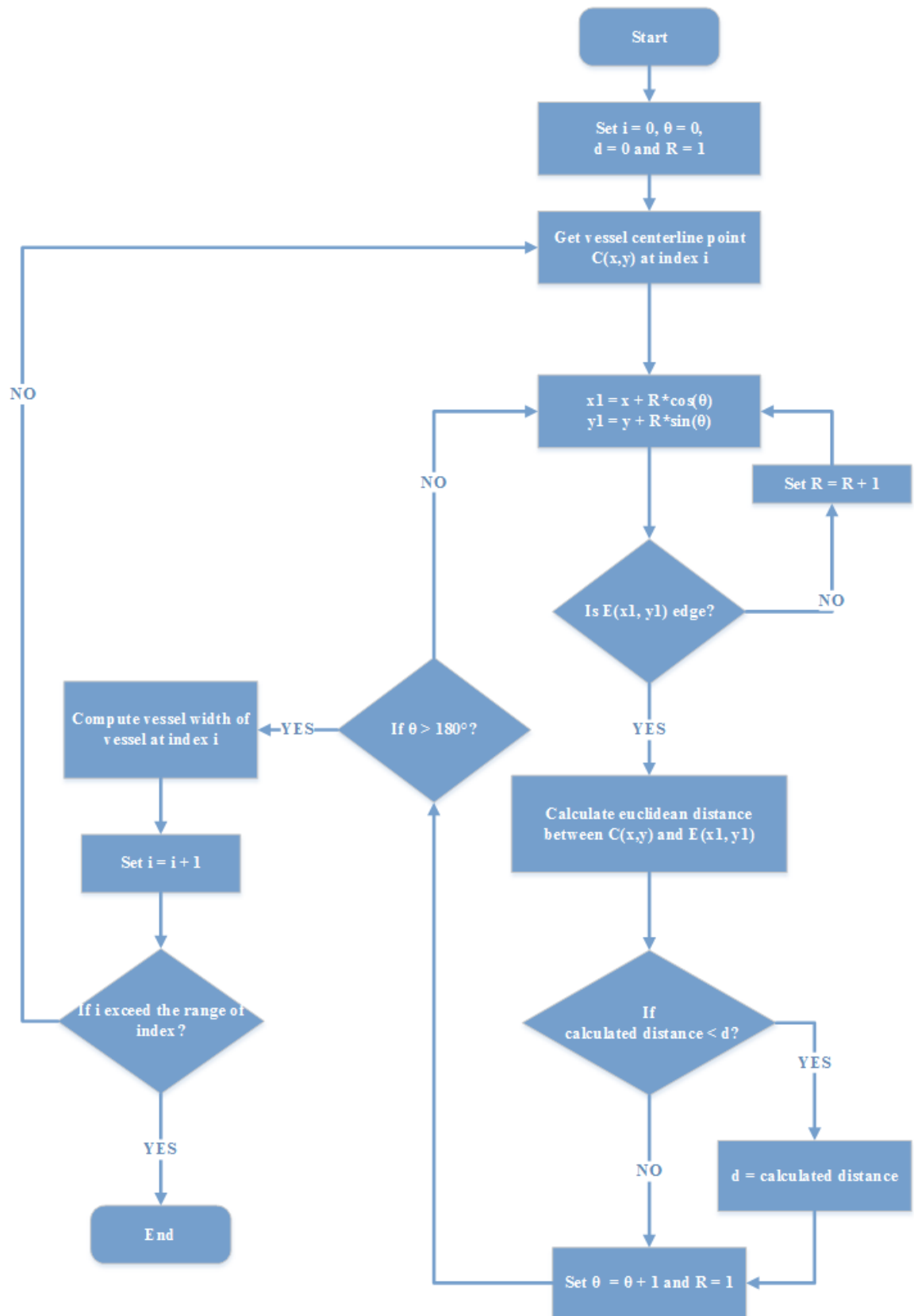


Figure 3.20 Flow diagram of vessel width calculation.

The major vessels were classified as artery or vein according to their calculated thicknesses. As a result of this classification, the AVR value which means the ratio of the retinal arteries to the retinal veins was calculated. Calculation of the AVR is based on the Parr- Hubbard formulas [6] which yield reliable results. AVR is found by the ratio of the Central Retinal Artery Equivalent (CRAE) to Central Retinal Vein Equivalent (CRVE). In equation 3.13 CRAE is calculated with the equation 3.13a where W_a is the caliber of the smaller branch of the arteriole and W_b is the caliber of the larger branch arteriole. In equation 3.13b CRVE is defined where W_a is the caliber of the smaller branch of the venules and W_b is the caliber of the larger branch venules.

$$AVR = \frac{CRAE}{CRVE} \quad (3.13)$$

$$CRAE = (0.87W_a^2 + 1.01W_b^2 - 0.22W_aW_b - 10.73)^{\frac{1}{2}} \quad (3.13a)$$

$$CRVE = (0.72W_a^2 + 0.91W_b^2 + 450.02)^{\frac{1}{2}} \quad (3.13b)$$

In this thesis with the help of these formulas, AVR was calculated simply by proportion of caliber of arteries to caliber of veins. After determining AVR, the last step was to identify the presence of the hypertensive retinopathy. Keith-Wagener-Barker gives AVR value for the presence of HR [58]. The grading of HR was shown in the Table 3.1. According to this table, in this thesis retina image was marked as HR if AVR is smaller than 0.667 or was marked as non-HR if AVR value is between 0.667 and 0.75.

Table 3.1 Keith-Wagener-Barker AVR values to diagnose HR.

Presence of HR	AVR Value
Non- HR	0.667 – 0.75
HR	< 0.667

CHAPTER 4

RESULTS AND DISCUSSION

In this section, the test results of the steps of diagnosis of hypertensive retinopathy that were described in detail in the implementation section have been shared. Tests were performed on images from DRIVE and STARE databases. As a result, it has been shown that hypertensive retinopathy can be diagnosed with high accuracy and high processing speed. The results of the application were examined in 4 different groups. They are as follows;

- Blood vessel segmentation
- Detection of optic disc location
- Diagnosis of hypertensive retinopathy
- GPU optimized results

4.1 Blood Vessel Segmentation

Proper operation of the segmentation of blood vessels greatly affects the overall operation of the hypertensive retinopathy diagnosis system. Because measurement of vessels thickness and classification of them have been done on segmented images. Therefore, it was aimed to achieve high accuracy. As mentioned in the implementation chapter, average filter and thresholding method have been used for segmentation of blood vessels. The implemented method was evaluated on 20 images from the DRIVE database and 20 images from the STARE database. In evaluation the results, manually segmented images were used which are provided by DRIVE and STARE. The segmented images that were obtained implemented method were compared with manually segmented images pixel by pixel. To calculate performance of the comparison statistically, sensitivity in (4.1), specificity in (4.2) and accuracy in (4.3) parameters were calculated separately for all images.

- Sensitivity (true positive rate) measures the percentage of correctly identified vessel pixels (white pixels).

- Specificity (true negative rate) measures the percentage of correctly identified non-vessel pixels (black pixels)
- Accuracy is ratio of the total number of correctly classified pixels by total number of pixels.

$$Sensitivity = \frac{TP}{TP+FN} \quad (4.1)$$

$$Specificity = \frac{TN}{TP+FN} \quad (4.2)$$

$$Accuracy = \frac{TP+TN}{TP+TN+FP+FN} \quad (4.3)$$

To calculate these three performance measures, parameters that were shown in Table 4.1 is used where true positive (TP) indicates the correctly identified vessel pixels, true negative (TN) is correctly identified non-vessel pixels, false positive (FP) indicates the incorrectly identified vessel pixels and false negative (FN) indicates incorrectly identified non-vessel pixels.

Table 4.1 Parameters of performance measures.

	Correctly identified	Incorrectly identified
Vessel pixel	True Positive (TP)	False Positive (FP)
Non-vessel pixel	True Negative (TN)	False Negative (FN)

Statistical results for all images in DRIVE database were given in Table 4.2. When the results were examined, it was shown that this implemented method worked with approximately %95 accuracy and %97 specificity. It was seen that these two performance measures were same when they were compared with the performance measures of manually segmented images by human observer. In addition, the human observer achieved %78 sensitivity, while with the segmentation that conducted within the scope of the thesis yielded %66 sensitivity. Sensitivity rate of overall blood vessel segmentation was ignored, because the blood vessels around the optic disc were used for further operations. So, this obtained sensitivity value was enough for well separation of blood vessels in optic disc area.

Table 4.2 Accuracy calculations for all images from DRIVE database.

Images	Sensitivity	Specificity	Accuracy
1	0.6848	0.9842	0.9575
2	0.6025	0.991	0.9512
3	0.6463	0.9624	0.9309
4	0.6024	0.9886	0.953
5	0.6477	0.9598	0.9306
6	0.612	0.9714	0.9364
7	0.656	0.9508	0.9238
8	0.6062	0.9717	0.9403
9	0.6272	0.9762	0.9479
10	0.6847	0.9328	0.9124
11	0.6426	0.9754	0.9456
12	0.6717	0.9747	0.9485
13	0.6202	0.9835	0.948
14	0.6884	0.9737	0.9506
15	0.7298	0.9573	0.941
16	0.6703	0.9882	0.9595
17	0.6058	0.9832	0.9514
18	0.7112	0.9688	0.9484
19	0.7966	0.9819	0.9666
20	0.7299	0.9733	0.9554
Average	0.6618	0.9725	0.9449
Human Observer	0.7763	0.9723	0.9470

4.2 Detection of Optic Disc Location

Accurate detection of the location of the optic disc as well as the success achieved from blood vessel segmentation plays an important role in the diagnosis of hypertensive retinopathy with high accuracy. The code developed to find the optic disc radius and center point was applied on 20 images that are taken from the DRIVE database. Optic disc region was marked on the original image based on the radius and center point information. The results that were produced in the application were compared manually. As a result of this comparison, while the optic disc location was successfully detected at 18 out of 20 images, the optic disc location could not be clearly determined in the remaining 2 images. The success rate of this step according to obtained results was calculated as %90. Figure 4.1 shows result of all test images that were detected correctly or incorrectly.

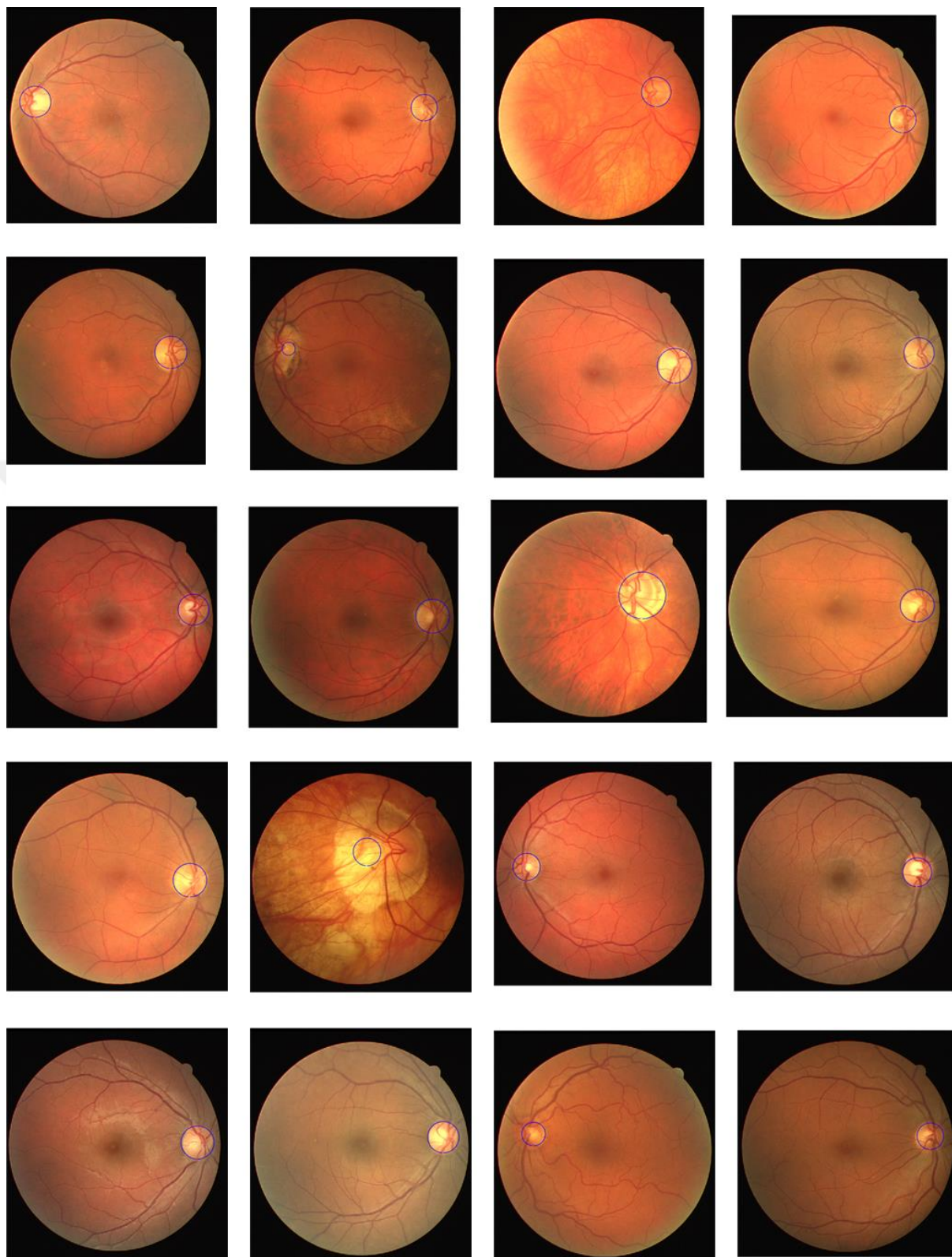


Figure 4.1 Optic disc detection results for images from DRIVE database.

4.3 Diagnosis of Hypertensive Retinopathy

The ability to diagnose hypertensive retinopathy with a high success rate is greatly influenced by the success of other steps. As the last step of this study, the classification of HR was made according to the calculated AVR values for images that are taken from the STARE database. In the images that were used to test, 26 retinal images are diagnosed as a HR. In addition, 41 retinal images are label as a normal, ie healthy.

As a result of the application, 18 images of the 26 images that are labelled as HR were correctly classified. In the remaining 8 images, HR diagnosis was not performed correctly. Therefore %69 success rate was obtained for HR classification. Moreover, 35 of the 41 healthy images were correctly classified as a normal and correct decision was not made for the remaining images. %85 success rate was obtained for this trial. These results can be seen in Figure 4.2 and Figure 4.3.

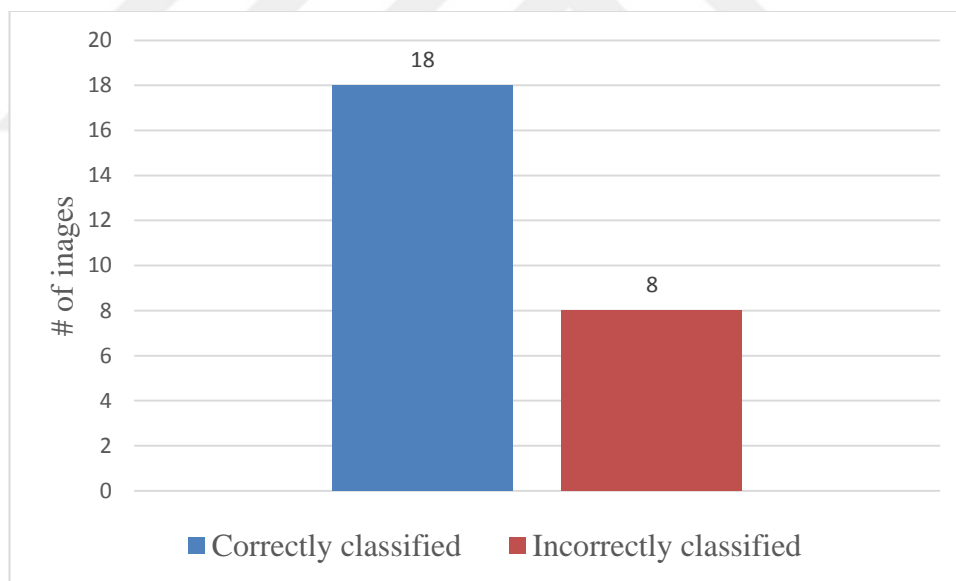


Figure 4.2 Classification result for images labelled as HR in STARE database.

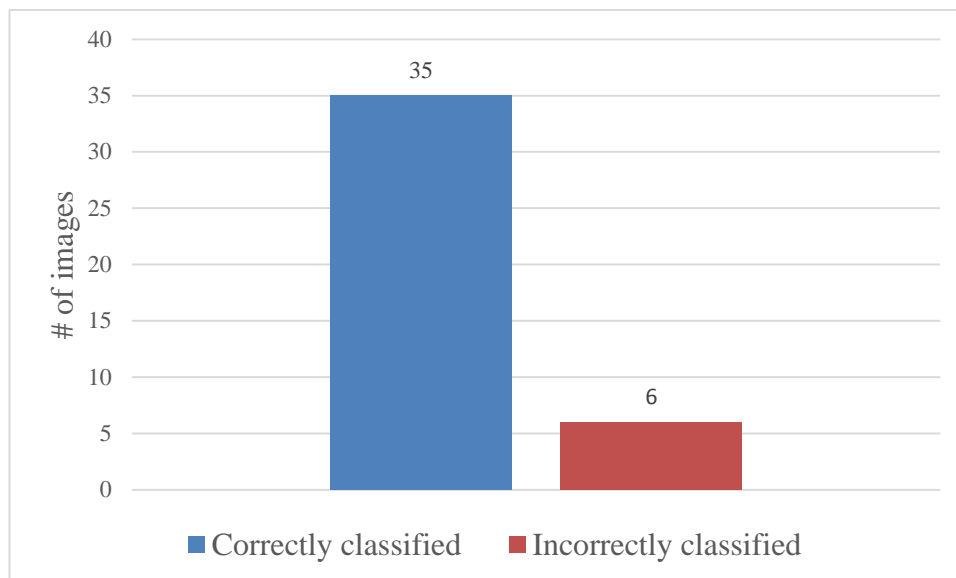


Figure 4.3 Classification result for images labelled as normal (non-HR) in STARE database.

4.4 GPU Optimized Results

The main objective of this thesis is to be able to diagnose hypertensive retinopathy with high speed and high accuracy. The implementations on the CPU have shown that the diagnosis has been made with high accuracy. Without sacrificing this accuracy, the high performance of the algorithm has been provided by the GPU. CPU and GPU run times have been compared for pre-processing, segmentation and detection of optic disc location steps which could be made parallel with MATLAB `gpuArray`. For a single image, it has been observed that CPU and GPU run times were very close to each other. However, it has been observed that the solution applied on the GPU was better than the solution applied on the CPU when an input image with a higher resolution was processed or when the application had a higher processing load.

In order to be able to perform the performance measurement in a healthy way, the application has been tested on N number of images repeatedly. By testing in this way, the processing load of the application has been increased controllably and processing times have been measured each time. The measured processing times on CPU and GPU for different situations have been shown in the graph in Figure 4.4. It

has been seen that implementation accelerate up to 8 times in applications on the current GPU.

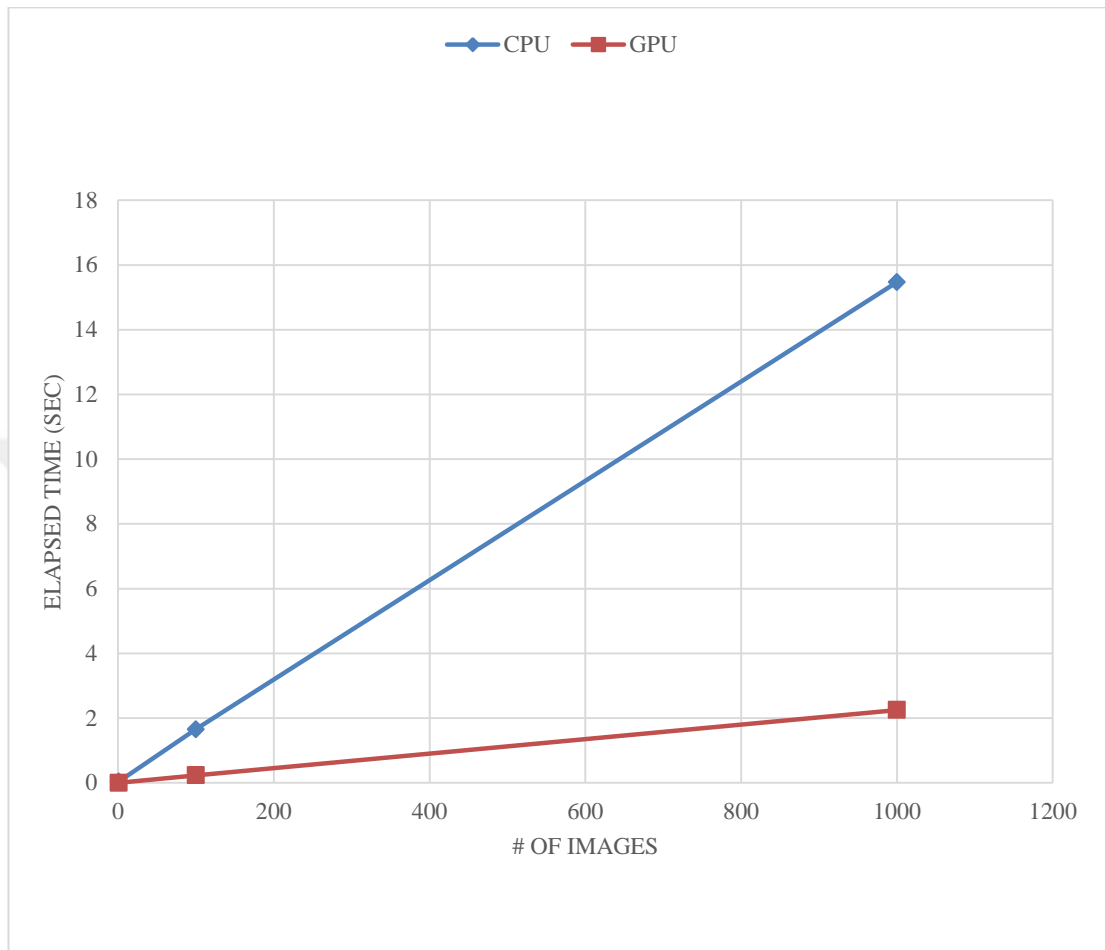


Figure 4.4 The graphical representation of running times on GPU and CPU.

CHAPTER 5

CONCLUSION AND FUTURE WORKS

It is known that eye diseases such as hypertensive retinopathy and diabetic retinopathy can cause severe damage to the human body. These types of diseases can lead to vision loss when they reach advanced levels. Therefore, accurate early detection of these diseases is important for timely treatment. In addition, the examination of retinal images with computerized systems at high speed and minimum error provides great convenience for ophthalmologists.

In this study, it was aimed to diagnose and detect hypertensive retinopathy with high speed and high accuracy. One of the most prominent indicators of hypertensive retinopathy is arterial narrowing. Determination of arterial narrowing is done by calculating AVR value which is a ratio of thicknesses arteries to thicknesses veins. The algorithm developed in this study was applied on images which were taken from publicly available DRIVE and STARE databases. As the first step, a number of image enhancement techniques were applied to retinal images for effective blood vessel segmentation. Then, optic disc was determined to identify region of interest in which vessels would be examined. Major vessels were detected separately and thicknesses of them were calculated. According this calculation vessels were classified as arteries and veins and final AVR value was calculated. Presence of the hypertensive retinopathy was decided with respect to the AVR. It was seen that the decision was executed with high accuracy. Besides achieving high accuracy, one of the main purposes of the thesis was to accelerate the methods with long processing time with the help of GPU computing. The GPU were applied to the pre-processing, segmentation and finding optic disc steps which were the main steps of the thesis. It was seen that the GPU processing time was 8 times faster than the CPU processing times. Finally, the presence of hypertensive retinopathy has been detected with high performance without sacrificing accuracy.

In addition, the academic paper entitled “Segmentation of Blood Vessels in 2D Retinal Images with Graphical Processing Units” that describes the details of the

segmentation step of this thesis has been presented at the conference of “25th Signal Processing and Communications Applications Conference, Antalya 2017 (SIU 2017)”. In this paper, was shown that retinal images that are taken from the DRIVE database were detected with an average accuracy rate of %96 and 7x speedup with GPU implementation [59].

Although the application that has been developed under the thesis can work with high accuracy and high performance, both the accuracy and the performance of the application can be increased by a number of joints to be implemented in the future. Firstly, the classification of blood vessels was done according to only their thicknesses. However, the classification that is based on a single feature is open to misclassification. The measured thickness information of the not well segmented vessels may give erroneous results. So, if different features of the artery and vein are provided by eye specialists in the future, features can be extracted by extraction methods and according to these extracted features separation of vessels can be done with classification algorithms like Support Vector Machine. When the vessels are classified more precisely, the accuracy of the measured AVR will increase accordingly. Therefore, the diagnosis of hypertensive retinopathy can be made more exactly and even it can be graded.

Furthermore, in terms of performance of the application, each step of the algorithm that was developed was not parallelized. Primarily, the performance of this system will increase when steps that take long processing time are parallelized. In addition, the results that are obtained on the GPU may vary depending on the characteristics of the GPU machine and also the properties of the image to be processed such as size of it. If these improvements had been made with better graphics cards, the performance results would definitely better than results that were obtained in this work.

In addition, MATLAB GPU built-in functions were used to parallelize algorithms steps. So when the functions that MATLAB does not support and the algorithms written by us are parallelized, the performance of the application will increase. Obviously, this way will have shared and global memory usage, which will be effective in increasing performance.

REFERENCES

- [1] Informed Health Online [Internet], "*How does the eye work?* [online]", Cologne, Germany: Institute for Quality and Efficiency in Health Care (IQWiG), <https://www.ncbi.nlm.nih.gov/books/NBK279248/>, [Accessed: 24-Apr-2017].
- [2] Patton Niall., & Aslam Tariq M., & MacGillivray Thomas., & Deary Ian J., & Dhillon Baljean., & Eikelboom Robert H., & Yogesan Kanagasingham., & Constable Ian J., "*Retinal image analysis: Concepts, applications and potential*", *Progress in Retinal and Eye Research*, 25 (1), 99–127, 2006.
- [3] Chaudhuri Subhasis., & Chatterjee Shankar., & Katz Norman., & Nelson Mark., & Goldbaum Michael, "*Detection of blood vessels in retinal images using two-dimensional matched filters*", *IEEE Transactions on Medical Imaging*, 8 (3), 263–269, 1989.
- [4] Wong Tien Yin., & McIntosh Rachel, "*Hypertensive retinopathy signs as risk indicators of cardiovascular morbidity and mortality*", *Br. Med. Bull.*, 73–74, 57–70, 2005.
- [5] Garner A., & Ashton N., "*Pathogenesis of hypertensive retinopathy: a review*", *Journal of the Royal Society of Medicine*, 72 (5), 362–365, 1979.
- [6] L. D. Hubbard, R. J. Brothers, W. N. King, L. X. Clegg, R. Klein, L. S. Cooper, a R. Sharrett, M. D. Davis, and J. Cai, "*Methods for evaluation of retinal microvascular abnormalities associated with hypertension/sclerosis in the Atherosclerosis Risk in Communities Study*", *Ophthalmology*, vol. 106, no. 12, pp. 2269–2280, 1999.
- [7] C. Kondermann, D. Kondermann, and M. Yan, "*Blood vessel classification into arteries and veins in retinal images*", *Image Processing*, p. 651247, 2007.
- [8] G. C. Manikis, V. Sakkalis, X. Zabulis, P. Karamaounas, A. Triantafyllou, S. Douma, C. Zamboulis, and K. Marias, "*An Image Analysis Framework for the*

- Early Assessment of Hypertensive Retinopathy Signs*”, Proc. 3rd Int. Conf. E-Health Bioeng. - EHB, pp. 413–418, 2011.
- [9] M. R. Faheem and Mui-zzud-Din, “*Diagnosing Hypertensive Retinopathy through Retinal Images*”, Biomed. Res. Ther., vol. 2, no. 10, p. 25, Nov. 2015.
- [10] K. Noronha, K. . Navya, and N. K. Prabhakar, “*Support System for the Automated Detection of Hypertensive Retinopathy using Fundus Images*”, Int. Conf. Electron. Des. Signal Process., pp. 7–11, 2012.
- [11] U. G. Abbasi and M. Usman Akram, “*Classification of blood vessels as arteries and veins for diagnosis of hypertensive retinopathy*”, 10th International Computer Engineering Conference (ICENCO), pp. 5–9, 2014.
- [12] K. Narasimhan, V. C. Neha, and K. Vijayarekha, “*Hypertensive Retinopathy Diagnosis from Fundus Images by Estimation of Avr.*,” *Procedia Eng.*, vol. 38, pp. 980–993, 2012.
- [13] J. Lowell, A. Hunter, D. Steel, A. Basu, R. Ryder, and R. L. Kennedy, “*Measurement of retinal vessel widths from fundus images based on 2-D modeling*”, IEEE Trans. Med. Imaging, vol. 23, no. 10, pp. 1196–1204, 2004.
- [14] C. Muramatsu, Y. Hatanaka, T. Iwase, T. Hara, and H. Fujita, “*Automated detection and classification of major retinal vessels for determination of diameter ratio of arteries and veins*,” Proc. SPIE 7624, Med. Imaging 2010 Comput. Diagnosis, vol. 7624, p. 76240J, 2010.
- [15] D. Ortiz, M. Cubides, A. Suarez, M. Zequera, J. Quiroga, J. Gomez, and N. Arroyo, “*Support system for the preventive diagnosis of Hypertensive Retinopathy*”, 2010 Annual International Conference of the IEEE Engineering in Medicine and Biology, pp. 5649–5652, 2010.
- [16] C. Agurto, V. Joshi, S. Nemeth, P. Soliz, and S. Barriga, “*Detection of hypertensive retinopathy using vessel measurements and textural feature*”, 2014 36th Annual International Conference of the IEEE Engineering in Medicine and Biology Society, 2014, vol. 2014, pp. 5406–5409.

- [17] F. Argüello, D. L. Vilariño, D. B. Heras, and A. Nieto, “*GPU-based segmentation of retinal blood vessels*”, *J. Real-Time Image Process.*, 2014.
- [18] G. S. Torres, J. A. Taborda, and U. Magdalena, “*Optic Disk Detection and Segmentation of Retinal Images Using an Evolution Strategy on GPU*”, *Symposium of Signals, Images and Artificial Vision - 2013*, pp. 1-5, 2013.
- [19] A. A. Jose, Y. P. Singh, and S. Patel, “*Retinal Fundus Image Enhancement using accelerated parallel implementation on GPU*”, *International Journal of Engineering Research and General Science*, vol. 3, no. 3, pp. 657–660, 2015.
- [20] J. Staal, M. D. Abramoff, M. Niemeijer, M. A. Viergever, and B. van Ginneken, “*Ridge-Based Vessel Segmentation in Color Images of the Retina*”, *IEEE Trans. Med. Imaging*, vol. 23, no. 4, pp. 501–509, Apr. 2004.
- [21] M. M. Fraz, P. Remagnino, A. Hoppe, B. Uyyanonvara, A. R. Rudnicka, C. G. Owen, and S. A. Barman, “*Blood vessel segmentation methodologies in retinal images - A survey*” *Comput. Methods Programs Biomed.*, vol. 108, no. 1, pp. 407–433, 2012.
- [22] A. Hoover, V. Kouznetsova, and M. Goldbaum, “*Locating blood vessels in retinal images by piecewise threshold probing of a matched filter response*” *IEEE Trans. Med. Imaging*, vol. 19, no. 3, pp. 203–210, Mar. 2000.
- [23] S. Johnson, “*Stephen Johnson on Digital Photography*”, O’Reilly Media, Incorporated, 2006.
- [24] R. Gonzalez and R. Woods, “*Digital image processing*” 2002.
- [25] Y. Zhu and C. Huang, “*An Adaptive Histogram Equalization Algorithm on the Image Gray Level Mapping*” *Phys. Procedia*, vol. 25, pp. 601–608, 2012.
- [26] “Wikipedia Histogram Equalization.” [online]. https://en.wikipedia.org/wiki/Histogram_equalization, [Accessed: 24-Apr-2017].

- [27] H. Yoon, H., Han, Y., Hahn, “*Image Contrast Enhancement based Sub-histogram Equalization Technique without Over-equalization Noise*”, World Acad. Sci. Eng. Technol., vol. 3, no. 2, pp. 323–329, 2009.
- [28] S. Pizer, E. P. Amburn, J. D. Austin, R. Cromartie, A. Geselowitz, T. Greer, B. T. H. Romeny, J. B. Zimmerman, K. Zuiderveld “*Adaptive Histogram Equalization and Its Variations*”, Computer Vision, Graphics, and image processing, 39, pp. 355–368, 1987.
- [29] S. K. Shome, S. Ram, and K. Vadali, “*Enhancement of Diabetic Retinopathy Imagery Using Contrast Limited Adaptive Histogram Equalization*”, Int. J. Comput. Sci. Inf. Technol., vol. 2, no. 6, pp. 2694–2699, 2011.
- [30] Spatial Filters- Mean Filter, “*Mean Filter* [online].” <http://homepages.inf.ed.ac.uk/rbf/HIPR2/mean.htm>, [Accessed: 24-Apr-2017].
- [31] M. S. Mabrouk, N. H. Solouma, and Y. M. Kadah, “*Survey of Retinal Image Segmentation and Registration*,” GVIP J., vol. 6, no. 2, p. 1, 2006.
- [32] L. Tramontan, E. Grisan, and A. Ruggeri, “*An improved system for the automatic estimation of the arteriolar-to-venular diameter ratio (AVR) in retinal images*”, Conf. Proc. IEEE Eng. Med. Biol. Soc., vol. 2008, pp. 3550–3553, 2008.
- [33] J. Serra, “*Image Analysis and Mathematical Morphology*” Orlando, FL, USA: Academic Press, Inc., 1983.
- [34] R. M. Haralick, S. R. Sternberg, and X. Zhuang, “*Image Analysis Using Mathematical Morphology*” IEEE Trans. Pattern Anal. Mach. Intell., vol. 9, no. 4, pp. 532–550, 1987.
- [35] J. Prewitt, “*Object enhancement and extraction*”, Picture processing and Psychopictorics. 1970.
- [36] I. Sobel, “*Camera models and machine perception*,” Thesis (PhD), PhD dissertation Stanford Univ Stanford Calif. 1970.

- [37] J. Canny, “*A Computational Approach to Edge Detection*”, IEEE Trans. Pattern Anal. Mach. Intell., vol. PAMI-8, no. 6, pp. 679–698, 1986.
- [38] R. Maini and H. Aggarwal, “*Study and comparison of various image edge detection techniques*”, Int. J. Image Process., vol. 3, no. 1, pp. 1–11, 2009.
- [39] A. Gopalakrishnan, A. Almazroa, K. Raahemifar, V. Lakshminarayanan, and A. Preprocessing, “*Optic Disc Segmentation using Circular Hough Transform and Curve Fitting*”, Opto-Electronics and Applied Optics (IEM OPTRONIX), 2015, vol. 1, 2015.
- [40] S. Sekhar, W. Al-Nuaimy, and A. K. Nandi, “*Automated localisation of retinal optic disc using hough transform*”, 2008 5th IEEE Int. Symp. Biomed. Imaging From Nano to Macro, Proceedings, ISBI, pp. 1577–1580, 2008.
- [41] X. Zhu and R. M. Rangayyan, “*Detection of the optic disc in images of the retina using the Hough transform*”, Conf. Proc. ... Annu. Int. Conf. IEEE Eng. Med. Biol. Soc. IEEE Eng. Med. Biol. Soc. Annu. Conf., vol. 2008, pp. 3546–9, 2008.
- [42] P. V. C. Hough, “*Method and means for recognizing complex patterns*” US Pat. 3,069,654, 1962.
- [43] R. O. Duda and P. E. Hart, “Use of the Hough transformion to detect lines and curves in pictures,” *Commun. Assoc. Comput. Mach.*, vol. 15, no. 1, pp. 11–15, 1972.
- [44] “MATLAB: Image Processing Toolbox Features.” [Online]. Available: <https://www.mathworks.com/products/image/features.html>. [Accessed: 24-Apr-2017]
- [45] “Introduction to Parallel Computing.” [Online]. Available: https://computing.llnl.gov/tutorials/parallel_comp/. [Accessed: 24-Apr-2017].
- [46] J. D. Owens, M. Houston, D. Luebke, S. Green, J. E. Stone, and J. C. Phillips, “GPU Computing,” *Proc. IEEE*, vol. 96, no. 5, pp. 879–899, May 2008.

- [47] J. Fung and S. Mann, "Using graphics devices in reverse: GPU-based Image Processing and Computer Vision," in *2008 IEEE International Conference on Multimedia and Expo*, 2008, pp. 9–12.
- [48] A. Georgantzoglou, J. da Silva, and R. Jena, "Image Processing with MATLAB and GPU," in *MATLAB Applications for the Practical Engineer*, InTech, 2014, pp. 623–653.
- [49] "Illustrating Three Approaches to GPU Computing: The Mandelbrot Set." [Online]. Available: <https://www.mathworks.com/help/distcomp/examples/illustrating-three-approaches-to-gpu-computing-the-mandelbrot-set.html>.
- [50] N. Otsu, "A threshold selection method from gray-level histograms," *IEEE Trans. Syst. Man. Cybern.*, vol. 9, no. 1, pp. 62–66, 1979.
- [51] S. Ridler, T.W. Calvard, "Picture Thresholding Using an Iterative Selection Method," *IEEE Trans. Syst. Man Cybern.*, vol. 8, no. 8, pp. 630–632, 1978.
- [52] C. Sinthanayothin, J. F. Boyce, H. L. Cook, and T. H. Williamson, "Automated localisation of the optic disc, fovea and retinal blood vessels from digital color fundus images," *Br. J. Ophthalmol.*, vol. 4, no. 83, pp. 902–910, 1999.
- [53] N. Nakajima and A. Taguchi, "A novel color image processing scheme in HSI color space with negative image processing," *2014 Int. Symp. Intell. Signal Process. Commun. Syst. ISPACS 2014*, no. 1, pp. 29–33, 2014.
- [54] R. Gonzalez and R. Woods, *Digital image processing*. 2002.
- [55] M. D. Knudtson, K. E. Lee, L. D. Hubbard, T. Y. Wong, R. Klein, and B. E. Klein, "Revised formulas for summarizing retinal vessel diameters", *Curr. Eye Res.*, vol. 27, no. 3, pp. 143–149, 2003.
- [56] C. Muramatsu, Y. Hatanaka, T. Iwase, T. Hara, and H. Fujita, "Automated selection of major arteries and veins for measurement of arteriolar-to-venular

diameter ratio on retinal fundus images”, *Comput. Med. Imaging Graph.*, vol. 35, no. 6, pp. 472–480, 2011.

- [57] Q. Mirsharif, F. Tajeripour, and H. Pourreza, “*Automated characterization of blood vessels as arteries and veins in retinal images*”, *Comput. Med. Imaging Graph.*, vol. 37, no. 7–8, pp. 607–617, Oct. 2013.
- [58] N. M. Keith, H. P. Wagener, and N. W. Barker, “*Some different types of essential hypertension: their course and prognosis.*,” *Am. J. Med. Sci.*, vol. 268, no. 6, pp. 336–45, Dec. 1974.
- [59] Akça, Z.; Şen, B., Akça E., “*Segmentation of Blood Vessels in 2D Retinal Images with Graphical Processing Units*”, *Signal Processing and Communications Applications Conference, SIU 2017, Antalya*.

RESUME

Zülbiye AKÇA

Place of birth: Ankara

Date of birth: 26/05/1989

E-mail: zulbiyeuyar89@gmail.com

EDUCATION

MSc, 2017, Department of Computer Engineering, Ankara Yıldırım Beyazıt University, Ankara, Turkey. GPA: 3.50/4.00. Thesis: High Performance Automated Diagnosis System for Hypertensive Retinopathy.

BS, 2012, Department of Electronic and Communication Engineering, Çankaya University, Ankara, Turkey. GPA: 3.81/4.00

BS, 2012, Department of Computer Engineering, Çankaya University, Ankara, Turkey (Double Major). GPA: 3.00/ 4.00

WORK EXPERIENCE

TÜBİTAK – Scientific Programs Assistant Expert (June 2013 -)

PUBLICATIONS

- 1) Akça, Z.; Şen, B., Akça E., "*Segmentation of Blood Vessels in 2D Retinal Images with Graphical Processing Units*", Signal Processing and Communications Applications Conference, SIU 2017, Antalya.